

Estrogen Receptor Modulators: Identification and Structure–Activity Relationships of Potent ER α -Selective Tetrahydroisoquinoline Ligands

Johanne Renaud,^{*,†} Serge François Bischoff,[‡] Thomas Buhl,[†] Philipp Floersheim,[‡] Brigitte Fournier,[†] Christine Halleux,[†] Joerg Kallen,[§] Hansjoerg Keller,[†] Jean-Marc Schlaeppli,[§] and Wilhelm Stark[§]

Novartis Pharma Research, WKL-136.3.25, CH-4002 Basel, Switzerland

Received February 19, 2003

As part of a program aimed at the development of selective estrogen receptor modulators (SERMs), tetrahydroisoquinoline derivative **27** was discovered by high throughput screening. Successive replacements of the *p*-F substituent of **27** by an aminoethoxy side chain and of the 1-H of the tetrahydroisoquinoline core by a 1-Me group provided analogues **19** and **20**. These compounds showed potencies in a cell-based reporter gene assay (ERE assay) varying between 0.6 and 20 nM and displayed antagonist behaviors in the MCF-7 human breast adenocarcinoma cell line with IC₅₀s in the range of 2–36 nM. The effect of *N*-phenyl substituents on the activity and pharmacokinetic properties of tetrahydroisoquinoline analogues was explored. As a result of this investigation, two potent derivatives bearing a *p*-F *N*-aryl group, **19c** and **20c**, were discovered as candidates suitable for further profiling. To gain insight into the ligand–receptor interaction, the X-ray crystallographic structure of the 1-H tetrahydroisoquinoline derivative (*R*)-**18a** in complex with ER α -ligand binding domain (LBD)_{301–553}/C→S triple mutant was solved to 2.28 Å. An overlay of this X-ray crystal structure with that reported for the complex of ER α -LBD_{301–553}/carboxymethylated C and raloxifene (**5**) shows that both compounds bind to the same cleft of the receptor and display comparable binding modes, with differences being observed in the conformation of their “D-ring” phenyl groups.

Introduction

Estrogens such as 17 β -estradiol (**1**) and estrone (**2**) (Figure 1) are steroid hormones long recognized as key mediators of female reproductive functions. However, they also exert their actions on other systems. For instance, estrogens contribute to the maintenance of bone tissue by determining the rate at which bone is renewed through a process involving bone resorption and bone formation.¹ They influence bone remodeling by suppressing, either directly or indirectly, the production of a number of cytokines which regulate the formation of osteoclasts, the cells responsible for bone resorption.² Most endogenous estrogens bind with high affinity to the two currently known estrogen receptors, ER α and ER β .³ The two receptors, which act as ligand-activated transcription factors, are found in a wide variety of tissues and show a distinct but also overlapping distribution pattern.^{3,4} X-ray crystal structures of receptor–ligand complexes have shown that the binding pockets of ER α and ER β differ by only two amino acids (Leu and Met in ER α are replaced by Met and Ile in ER β),⁵ a feature which explains the lack of selectivity of 17 β -estradiol (**1**) in binding the estrogen receptors. Current evidence point toward ER α as occupying an important role in bone remodeling,⁶ but ER β may also be a contributor to this process.⁶ It is not yet clear what effect an ER subtype-selective ligand would trigger on bone tissue.

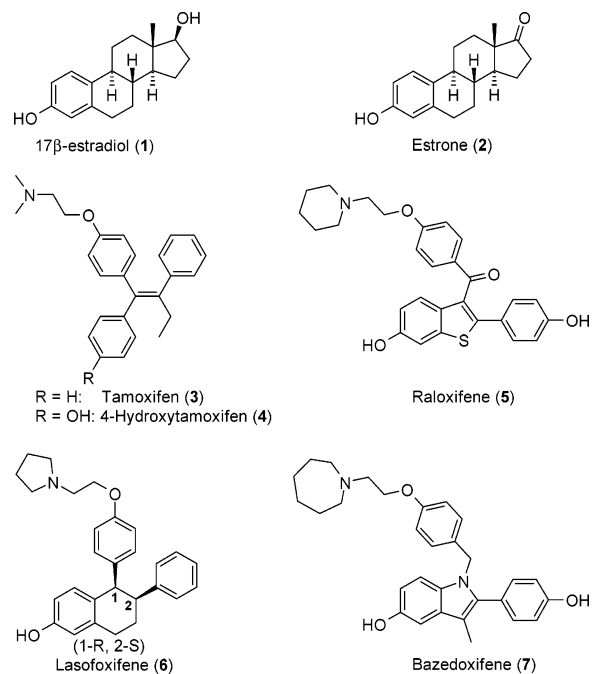


Figure 1. Structures of estrogens and SERMs.

It is apparent, however, that the decline in ovarian estrogen production which accompanies menopause causes an elevation in osteoclast number leading to an increase in bone remodeling.⁷ Since there is an imbalance between bone resorption and bone formation processes in favor of the former, the increase in bone turnover results in accelerated bone loss. This phenomenon gives rise to progressive thinning of cancellous and cortical bone structures and to a decrease of the me-

* To whom correspondence should be addressed. Tel: +41 61 696 5399. Fax: +41 61 696 6071. E-mail: johanne.renaud@pharma.novartis.com.

[†] Arthritis and Bone Metabolism Therapeutic Area.

[‡] Nervous System Therapeutic Area.

[§] Central Technologies.

chanical properties of the bone and its resistance to fractures.^{7,8} In addition to affecting bone metabolism, the reduction of endogenous estrogens levels caused by ovarian failure has been linked to the transient appearance of vasomotor symptoms such as hot flashes and night sweats and to changes in hepatic lipid metabolism.⁸

Hormone replacement therapies (estrogens alone or estrogens coadministered with progestins to oppose the stimulating action of estrogens on uterine tissue) have been used for the treatment of vasomotor symptoms related to the menopause and for prevention of osteoporosis.^{7,8} Additionally, these therapeutic regimens have been prescribed for the prevention of heart diseases since observational studies suggested that estrogens lower the risk of cardiovascular diseases.^{7,8b} However, the recent results of the Women's Health Initiative (WHI) study comparing oral administration of combined estrogens/progestin with placebo showed that women using the combination therapy experience increased risks of coronary heart disease and breast cancer.⁹ On the other hand, positive effects on fracture rates and reductions of colorectal cancer were reported.⁹

These results highlight the need to further develop surrogates able to effect bone protection in an estrogen-like manner without demonstrating its adverse side effects on breast, uterine tissues, and the cardiovascular system. Compounds which display such a tissue-selective behavior, mimicking estrogen in some tissues while antagonizing its action in others are named SERMs (selective estrogen receptor modulators)¹⁰ (Figure 1). A number of SERMs are currently in clinical trials and two compounds of this class, tamoxifen (**3**, its most active metabolite being 4-hydroxytamoxifen (**4**)) and raloxifene (**5**), are currently on the market for the treatment of hormone-dependent breast cancer^{10c,d} and prevention and treatment of osteoporosis,¹¹ respectively. These two products have distinct pharmacological profiles. Both compounds demonstrate bone-protective effects in humans, but tamoxifen (**3**) has been shown to increase the risk of endometrial cancer,^{10,12} while raloxifene (**5**) does not appear to be associated with uterine side effects.¹¹ Both tamoxifen (**3**) and raloxifene (**5**) have been linked to an increased risk of thromboembolism and to an exacerbation of hot flushes in a number of patients. In addition, the latter substance suffers from a low oral bioavailability in humans (2%).¹¹

The distinctive pharmacological behaviors of tamoxifen (**3**) and raloxifene (**5**) were postulated to be linked, in part, to the spatial orientation of their respective 2-aminoethoxyphenyl moiety relative to the plane of their central core. The phenyl group bearing the 2-aminoethoxy side chain in tamoxifen (**3**) is coplanar in relation to its stilbene skeleton, while that of raloxifene (**5**) is oriented orthogonally to the plane of its benzothiophene nucleus, an orientation rendered possible by the presence of the carbonyl functionality.¹³ In addition, the low bioavailability of raloxifene (**5**), which results from extensive phenolic glucuronidation in animals and in postmenopausal women, was hypothesized to stem from the planarity of its phenol-containing nucleus acting as a substrate for glucuronosyltransferases (UGTs).¹⁴ On the other hand, a compound such as lasofoxifene (**6**) embedding a less planar phenol

showed an improved bioavailability profile in rats and in monkeys (60% and 45%, respectively) compared with that displayed by raloxifene (**5**) in the same species (10 and 5%, respectively).¹⁴

In light of the subtle structural features that greatly influence SERMs' activity (on breast, uterine, bone tissues, and lipid metabolism) and bioavailability, we initiated a program aiming to identify new compounds of this class with improved pharmacological properties. We wish to disclose here the results of our initial efforts in the investigation of ER α -selective ligands of the tetrahydroisoquinoline series leading to the discovery of analogues which display excellent in vitro properties and have good bioavailabilities in rats.

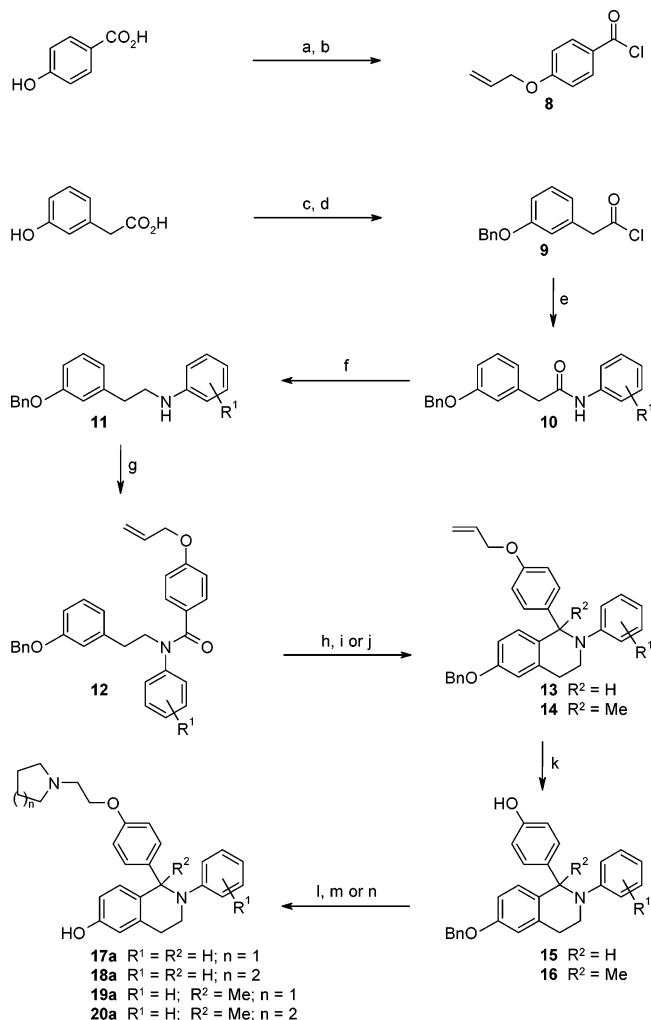
Chemistry

The tetrahydroisoquinolines were initially prepared via a route involving a Bischler–Napieralski cyclization reaction as outlined in Scheme 1.¹⁵ 3-Benzyloxyphenylacetyl chloride (**9**), prepared in two steps from 3-hydroxyphenylacetic acid, was transformed into the amide **10** by treatment with aniline. LAH-mediated reduction of **10** led to the aniline derivative **11** which, upon reaction with 4-allyloxybenzoyl chloride (**8**), furnished amide **12**. This latter compound was transformed into an intermediate iminium ion by the action of POCl₃ at reflux temperature. Conversion of this iminium ion into compounds **13** and **14** was achieved by reduction with NaBH₄ to produce the former or via reaction with MeMgBr in Et₂O to generate the latter.¹⁶ Pd(OAc)₂-catalyzed removal of the allyloxy protecting group provided phenols **15** and **16** which underwent alkylation upon treatment with NaH and 1-(2-chloroethyl)piperidine or 1-(2-chloroethyl)piperidine in dioxane. Deprotection yielded the final products **17a–20a**.

Aiming to shorten and improve the preparation of our final target molecules, we devised a second synthetic approach to products **19a–j**, **20a–j**, and **26a** as depicted in Scheme 2. In the first step of our new sequence, we made use of the Schmidt rearrangement of 5-methoxyindanone (**21**) to quickly and conveniently access large quantities of the bicyclic lactam **22**.¹⁷ The isoquinolin-1-one **22** proved to be a versatile intermediate of our synthetic scheme. It was cleanly and efficiently *N*-arylated under Ullmann-type conditions, using CuI in DMF.¹⁸ Compounds **23a–j** were then converted into the tetrahydroisoquinolines **24a–j** in two steps. Treatment of **23a–j** with benzyloxyphenyllithium provided, after acidic workup with HClO₄, intermediate iminium salts which were subsequently treated with MeMgBr in THF to furnish the desired 1-methyl-tetrahydroisoquinolines **24a–j**.¹⁶ AlCl₃-mediated debenzylation¹⁹ was carried out in the presence of Me₂NPh in CH₂Cl₂ to yield phenols **25a–j**. Alkylation of **25a–j** followed by cleavage of the methyl ether in the presence of AlCl₃ and EtSH provided tetrahydroisoquinolines **19a–j**, **20a–j**, and **26a** in a short sequence of steps.

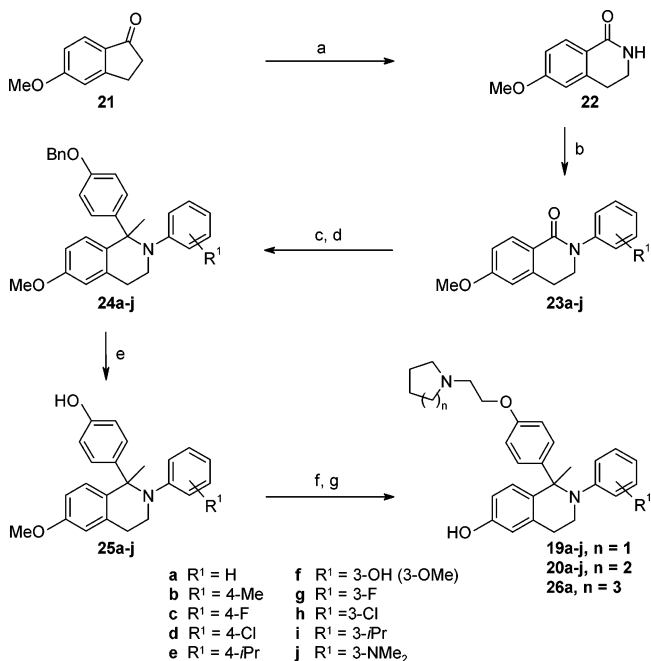
Biology

As part of our initial screening strategy, our compounds were tested in three in vitro assays. Binding to the estrogen receptor is a prerequisite in the search for compounds able to modulate estrogen signaling with SERM-like characteristics. Thus, in a first instance, the

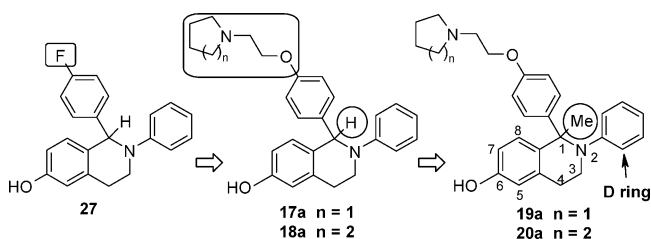
Scheme 1. Bischler–Napieralski Route to Tetrahydroisoquinolin-6-ol Derivatives^a


^a Reagents: (a) BrCH₂CH=CH₂ (1.05 equiv), KOH (2.5 equiv), NaI (0.014 equiv), EtOH (0.24 M), reflux, 20 h; HCl, 60%; (b) (COCl)₂ (1.5 equiv), CH₂Cl₂ (0.43 M), rt, 3 h, 91%; (c) BnBr (1.05 equiv), KOH (2.5 equiv), NaI (0.02 equiv), EtOH (0.22 M), reflux, 19 h; HCl, 90%; (d) (COCl)₂ (1.5 equiv), CH₂Cl₂ (0.29 M), 40 °C, 18 h, 100%; (e) PhNH₂ (1.5 equiv), Na₂CO₃ (3 equiv), PhH (0.073 M), reflux, 20 h, 68%; (f) LAH (3 equiv), dioxane–Et₂O (2:3), 40 °C, 17 h, 83%; (g) 4-allyloxybenzoyl chloride (**8**, 1.2 equiv), Na₂CO₃ (3 equiv), benzene (0.055 M), 2 h, reflux, 83%; (h) POCl₃ (30 equiv), reflux, 1.5 h; KI; (i) NaBH₄ (2.2 equiv), MeOH (0.27 M), rt, 1 h, 74% over two steps; (j) MeMgBr (1.5 equiv), Et₂O (0.26 M), reflux, 18 h, 79% over 2 steps; (k) for R = H: Ph₃P (1.5 equiv), morpholine (1.2 equiv), Pd(OAc)₂ (0.05 equiv), THF (0.19 M), rt, 18 h, 88%; for R = Me: Ph₃P (1.5 equiv), morpholine (1.5 equiv), Pd(OAc)₂ (0.10 equiv), THF (0.10 M), rt, 18 h, 51%; (l) NaH (2.0–3.9 equiv), 1-(2-chloroethyl)pyrrolidine·HCl (1 equiv) or 1-(2-chloroethyl)piperidine·HCl (1 equiv), dioxane (0.095–0.15 M), 80 °C, 8–22 h, 52–100%; (m) concd HCl, 90 °C, 1 h, 45–47%; (n) PhNMe₂ (10 equiv), AlCl₃ (3 equiv), CH₂Cl₂ (0.02 M), 2–6 h, 5–12%; Bn = benzyl; LAH = lithium aluminum hydride.

affinity/selectivity of the tetrahydroisoquinoline derivatives for ER α and ER β was evaluated in a [³H]-estradiol radioligand binding assay using recombinant human ER α and ER β . Potencies and selectivities were further assessed in a cellular transcription assay using HeLa cells stably transfected with human ER α and ER β and an estrogen response element (ERE) upstream of a luciferase gene. In view of the fact that hormones are key players in the regulation of target cell proliferation and protein syntheses and that estrogen administration

Scheme 2. The Schmidt Rearrangement Route to Tetrahydroisoquinolin-6-ols^a


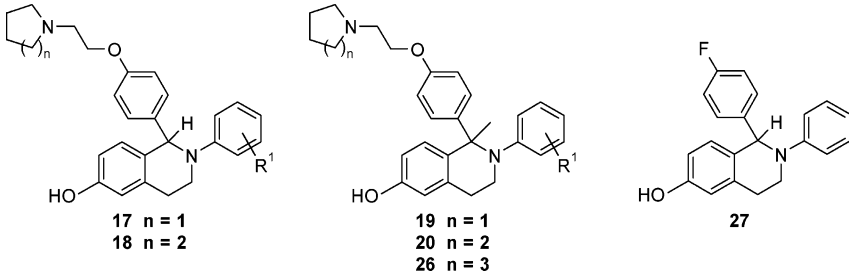
^a Reagents: (a) Reference 17; (b) ArI, CuI, K₂CO₃, DMF, 150 °C, 18.5–164 h, 48–95%; (c) [LiArOBn] (generated from *p*-BrArOBn or *p*-IArOBn and *n*-BuLi), THF, –78 °C, 0.75–3 h; HClO₄, 10 min; (d) MeMgBr, THF, 0 °C to rt, 0.75–3 h, 47–90% over two steps; (e) AlCl₃, Me₂NPh, CH₂Cl₂, rt, 1–1.5 h, 44–75%; (f) NaH, 1-(2-chloroethyl)pyrrolidine·HCl, 1-(2-chloroethyl)piperidine·HCl, or 1-(2-chloroethyl)azepane·HCl, dioxane or dioxane–DMF, 80 °C, 1–20 h; (g) EtSH, AlCl₃, CH₂Cl₂, rt, 0.5–2 h, 22–75%; Bn = benzyl; LAH = lithium aluminum hydride; THF = tetrahydrofuran.


Figure 2. Lead identification and optimization.

has been linked to adverse effects due to its proliferative action on some tissues, the third in vitro assay was used as an indicator of the ligand's behavior on tissues/cells affected by estrogen. For this purpose, new molecules were evaluated for their ability to antagonize 17 β -estradiol (**1**)'s proliferative action on MCF-7 breast tumor cells. The agonist action of the SERMs was also measured in this cellular assay in the absence of estrogen. Finally, to get early insight into the pharmacokinetic properties of interesting compounds, selected candidates were profiled in rats using cassette dosing experiments.

Results and Discussion

High throughput screening of our sample collection using a binding assay led to the identification of tetrahydroisoquinoline **27** (Figure 2), a substance which had been reported as an antiimplantation agent.¹⁵ Not unexpectedly, compound **27** lacked antagonist activity in the MCF-7 cellular assay despite its affinity for ER α (IC₅₀ = 285 nM, Table 1). The requirement for a

Table 1. ER Binding, Transcriptional Activation through ERE, and Inhibition of MCF-7 Cell Proliferation


entry	no.	R ¹	n	radioligand binding assay ^a		ERE assay ^b		MCF-7 assay ^b		
				ERα IC ₅₀ (nM)	ERβ IC ₅₀ (nM)	ERα IC ₅₀ (nM)	ERβ IC ₅₀ (nM)	IC ₅₀ (nM)	Agonism (%)	EC ₅₀ (nM)
1	27	-	-	285 ± 34	421 ± 5	n.d. ^c	n.d. ^c	>1000	100 ± 11	1
2	17a	H	1	21 ± 1	166 ± 44	10.7 ± 2.4	291 ± 223	29 ± 11	34 ± 8	≤0.10
3	18a	H	2	19 ± 6	346 ± 3	16.5 ± 3.0	289 ± 17	32 ± 14	37 ± 18	<0.15
4	19a	H	1	38 ± 2	227 ± 23	1.8 ± 0.4	83 ± 11.5	n.d. ^c	n.d. ^c	n.d. ^c
5	20a	H	2	29 ± 13	104 ± 2	2.6 ± 0.8	83 ± 10	4.0 ± 0.6	13 ± 4	<0.1
6	26a	H	3	56 ± 28	200 ± 22	1.5 ± 0.8	80 ± 7	6.0 ± 3.9	13 ± 12	<0.1
7	19b	<i>p</i> -Me	1	31 ± 2	354 ± 5	3.5 ± 1.1	448 ± 30	4.1 ± 2.1	14 ± 3	<0.1
8	20b	<i>p</i> -Me	2	28 ± 2	421 ± 19	2.9 ± 0.8	486 ± 5	4.0 ± 2.7	9 ± 4	<0.1
9	19c	<i>p</i> -F	1	31 ± 2	204 ± 20	1.6 ± 0.3	82 ± 34	3.5 ± 0.9	16 ± 6	<0.1
10	20c	<i>p</i> -F	2	38 ± 5	317 ± 46	1.9 ± 0.4	92 ± 1	6.0 ± 2.9	13 ± 2	<0.1
11	19d	<i>p</i> -Cl	1	27 ± 3	302 ± 36	3.3 ± 0.3	531 ± 23	6.2 ± 4.8	10 ± 1	<0.1
12	20d	<i>p</i> -Cl	2	35 ± 2	396 ± 26	3.1 ± 0.4	552 ± 29	5.2 ± 3.4	8 ± 5	<0.1
13	19e	<i>p</i> -iPr	1	44 ± 17	1974 ± 605	2.6 ± 0.8	4974 ^d	3.2 ± 1.3	10 ± 5	<0.1
14	20e	<i>p</i> -iPr	2	71 ± 28	3687 ± 1811	5.2 ± 2.4	4776 ± 208	3.4 ± 1.5	14 ± 16	<0.1
15	19f	<i>m</i> -OH	1	31 ± 5	190 ± 32	0.6 ± 0.5	33 ± 16	2.0 ± 0.3	15 ± 3	<0.1
16	20f	<i>m</i> -OH	2	34 ± 16	304 ± 59	0.7 ± 0.1	47 ± 6	2.0 ± 1.0	10 ± 9	<0.1
17	19g	<i>m</i> -F	1	39 ± 17	123 ± 42	3.0 ± 1.4	198 ± 54	3.8 ± 1.0	5 ± 4	<0.1
18	19h	<i>m</i> -Cl	1	66 ± 38	272 ± 32	2.9 ± 0.8	106 ± 1	7.0 ± 3.5	20 ± 11	<0.1
19	20h	<i>m</i> -Cl	2	49 ± 18	284 ± 10	4.5 ± 1.3	159 ± 43	8.0 ± 3.9	18 ± 13	<0.1
20	20i	<i>m</i> -iPr	2	46 ± 4	1105 ± 75	16.1 ± 7.0	492 ± 91	27 ± 14	16 ± 7	<0.4
21	19j	<i>m</i> -NMe ₂	1	94 ± 10	2205 ± 305	19.0 ± 3.9	2974 ^d	32 ± 20	19 ± 9	<0.5
22	20j	<i>m</i> -NMe ₂	2	71 ± 22	3110 ± 110	19.8 ± 3.7	2183 ± 1045	36 ± 4.0	18 ± 8	<0.5
23	5^e	-	-	22 ± 6	260 ± 70	2.4 ± 0.7	341 ± 71	1.4 ± 1.0	22 ± 9	0.02
24	6^e	-	-	4 ± 2	13 ± 12	3.1 ± 1.0	24 ± 1	2.3 ± 1.0	29 ± 12	0.02
25	3	-	-	n.d. ^c	n.d. ^c	622 ± 20	>1000	580 ± 160	42 ± 10	10
26	4	-	-	17 ^d	21 ^d	10.3 ± 7.7	32 ± 4	8.5 ± 8.0	31 ± 8	0.12
27	1	-	-	28 ± 13	24 ± 7	n.d. ^c	n.d. ^c	n.d. ^c	100	0.01

^a Average of two independent experiments run in triplicate. ^b Average of two to four independent experiments run either in duplicate or in triplicate except when indicated. ^c n.d.: not determined. ^d Average of three determinations issued from one experiment. ^e Tested as the HCl salt.

Table 2. Pharmacokinetic Data for Selected Compounds^a

entry	no.	oral BAV (%)	maximal blood concentration po dose-normalized (C _{max}) (nM)	total clearance (CL) (mL/min kg)	terminal half-life for elimination (t _{1/2}) (h)
1	17a	73 ± 20	55 ± 15	55.0 ± 3.0	3.0 ± 0.2
2	18a	42 ± 10	31 ± 7	51.9 ± 3.2	3.5 ± 0.2
3	20a	23 ± 4	5.2 ± 1.5	116.4 ± 11.4	5.2 ± 1.9
4	19c	53 ± 7	20 ± 3	45.2 ± 4.0	8.6 ± 0.4
5	20c	56 ± 11	16 ± 2	64.9 ± 4.0	7.1 ± 0.5
6	19f	15 ± 2	5.3 ± 2.1	129.7 ± 14.8	5.9 ± 3.3
7	5^b	22 ± 4	7.5 ± 2.3	157.7 ± 11.7	1.7 ± 0.2
8	6^b	38 ± 5	15.5 ± 5.3	55.7 ± 4.3	5.2 ± 0.6

^a Pharmacokinetic parameters calculated from blood levels after iv (1 mg/kg) and po (5 mg/kg) administration to conscious rats. ^b Tested as the HCl salt. BAV = bioavailability.

correctly positioned aminoethoxy side chain to confer SERMs their antagonist properties has precedents in the literature. With this concept in mind, derivatives **17a** and **18a** were synthesized.²⁰ Not only did both compounds show a much improved potency in the MCF-7 assay, displaying IC₅₀s in the order of 29 and 32 nM, respectively, but their affinity to ERα in the binding assay was also increased (IC₅₀s = 21 and 19 nM, for compounds **17a** and **18a**, respectively, Table 1, entries 2 and 3). To assess at an early stage of the program whether our leads were bioavailable, the pharmacokinetic profiles of **17a** and **18a** were evaluated in a cassette dosing experiment carried out in rats. The

pyrrolidine and piperidine derivatives showed 73 and 42% oral bioavailabilities, respectively (Table 2, entries 1 and 2). These encouraging in vitro results and pharmacokinetic properties convinced us to further optimize potency. Since the binding pocket of ER is rather hydrophobic, we reasoned that we might be able to achieve our objective by increasing the lipophilicity of the tetrahydroisoquinoline core. With this aim in mind, we envisaged to introduce an alkyl substituent at the 1-position of the tetrahydroisoquinoline nucleus. We hypothesized that the binding pocket of ER might accommodate the presence of a methyl group at that position. To the best of our knowledge, SERMs possess-

ing cyclic frameworks incorporating an aminoethoxyphenyl and an alkyl substituent at the 1-position have not been reported in the literature. However, there is a literature precedent showing that the presence of an additional methyl group at the 2-position is not prohibitive for binding to ER α . The tetrahydronaphthalene derivative ZM 189,154 (2-(4-hydroxyphenyl)-2-methyl-1-[9-(4,4,5,5,5-pentafluoropentane-1-sulfinyl)nonyl]-1,2,3,4-tetrahydronaphth-6-ol),²¹ embedding a 4-hydroxyphenyl and a methyl group at the 2-position, was described as a pure antiestrogen having high affinity for ER α .

To verify our assumption, we synthesized the tetrahydroisoquinoline **20a** and profiled it in our in vitro assays. This derivative was found to display good binding affinity for ER α and ER β , confirming that the presence of a 1-Me group was tolerated. However, the binding affinity of **20a** relative to **18a** was not improved but, interestingly, the former compound displayed 8- and 6-fold increase in activity over the latter in the MCF-7 and transcriptional activation through ERE cellular assays, showing IC_{50s} comparable to those of raloxifene (**5**) and lasofoxifene (**6**) (Table 1, entries 23 and 24). Others have also experienced a similar phenomenon whereby compounds showing comparable potencies in the binding assay were differentiated in the MCF-7 assay.²² The observed disparity of the results could stem from differences in the physicochemical properties of the substances tested, differences which would in turn affect cell permeability, intracellular compound concentration and thus potency. From a mechanistic point of view, another plausible rationale relates to the likelihood that subtle conformational differences of the ligand-receptor complexes might influence the nature of the interactions with the transcriptional machinery and thus the read-out of the cellular assays. For example, 4-hydroxytamoxifen (**4**) but not raloxifene (**5**) has been shown to recruit steroid receptor coactivator 1 (SRC-1) to ER α in endometrial cells,²³ although both compounds have similar affinities to ER α (Table 1). The results of the cellular assays were thus believed to be more relevant to the physiological situation and were later used as main indicators of potency.

We then endeavored to expand the series and explore the effects of *N*-aryl substituents on the activity, selectivity, and particularly on the pharmacokinetic behavior of the resulting analogues. Compounds bearing para- and meta-substituents were prepared following the routes outlined in Schemes 1 and 2. As may be inferred from the data listed in Table 1, a number of potent compounds with IC_{50s} ranging between 0.6 and 19.8 nM and 2.0–36 nM for the ERE and MCF-7 assays were synthesized, indicating that various substituents were tolerated. These results are in accordance with data reported previously for raloxifene analogues where the influence of different "D-ring" substituents on activity was studied.^{22b} The presence of a *m*-OH functionality led to a slight increase of potency in the cell assays (Table 1, entries 15 and 16), while the addition of a *m*-Pr or a *m*-NMe₂ group decreased activity in the three in vitro tests (Table 1, entries 20–22). Noticeably high selectivity for ER α over ER β in both the binding and in the ERE assays was observed for analogues bearing a *p*-iPr group. Tetrahydroisoquinolines **19e** and **20e** which

embed this substitution pattern show specificities of up to 50-fold for ER α over ER β (as measured in the in vitro radioligand binding assay) (Table 1, entries 13, 14).

In view of the fact that tamoxifen (**3**) and its most active metabolite 4-hydroxytamoxifen (**4**) display a dual antagonist/agonist behavior in the MCF-7 cell assay,²⁴ the potential of the tetrahydroisoquinolines to favor tumor cell proliferation (agonistic behavior) in the absence of 17 β -estradiol (**1**) was also evaluated. The tetrahydroisoquinoline derivatives **19a–g** and **20a–f** exhibited an agonist activity weaker than that displayed by their desmethyl analogues, **17a** and **18a**, raloxifene (**5**), lasofoxifene (**6**), and 4-hydroxytamoxifen (**4**) (Table 1). Taken together, the results of the MCF-7 assay show that a number of tetrahydroisoquinoline analogues are potent estrogen antagonists in this assay and only display weak agonism in the absence of estrogen. These data indicate that such compounds may have a potential for breast cancer prevention/treatment in vivo, a feature which is relevant when considering substituting hormone replacement therapy (HRT) by a SERM treatment.

Pharmacokinetic Properties. Having in hand SERMs with the desired functional activity, we selected candidates for further profiling in a PK cassette dosing experiment in rats. The pharmacokinetic parameters for designated analogues in comparison with the two reference compounds **5** and **6** are disclosed in Table 2. The tetrahydroisoquinoline derivative **20a** displayed a modest 23% absolute oral bioavailability (BAV) and a low peak plasma level (C_{\max} of 5.2 nM, po, dose-normalized) in contrast to its desmethyl analogue **18a** which reached 42% bioavailability and a C_{\max} value of 31 nM p.o. dose-normalized. The data obtained for the *m*-OH analogue **19f** paralleled those observed for **20a**. A major improvement was achieved with the two derivatives bearing a *p*-F on the *N*-phenyl ring. The absolute oral bioavailabilities for the pyrrolidine and piperidine analogues **19c** and **20c** were 53 and 56%, and peak plasma levels reached values of 20 and 16 nM, respectively. This increase in bioavailability may result from blockage of oxidative metabolism of the *N*-phenyl at the para-position, indicating that oxidation of **20a** may be the predominant pathway for metabolism over direct glucuronidation. The values found for **19c** and **20c** compare favorably with those obtained for lasofoxifene (**6**, Table 2, entry 8, BAV: 38%; C_{\max} : 15.5 nM) and were higher than those exhibited by raloxifene (**5**, Table 2, entry 7; BAV: 22%; C_{\max} : 7.5 nM).

X-ray Crystal Structure. To gain insight into the ligand-receptor interaction, we aimed to obtain the X-ray crystal structure of a tetrahydroisoquinoline derivative in complex with ER α -ligand binding domain (LBD). The preparation of the complex of ER α -LBD with a racemic mixture of **18a** was initially performed following published procedures.^{25,26} The ER α -LBD (residues 301–553) was overexpressed in *Escherichia coli*, purified by ligand-affinity chromatography and carboxymethylated. However, no suitable crystals of the resulting complex could be obtained. Mass spectrometry analysis revealed heterogeneous carboxymethylation of the cysteines. To overcome this problem, three solvent accessible cysteines (C381, C417, C530) were mutated to serines.²⁷ The complex of ER α -LBD mutant with **18a**

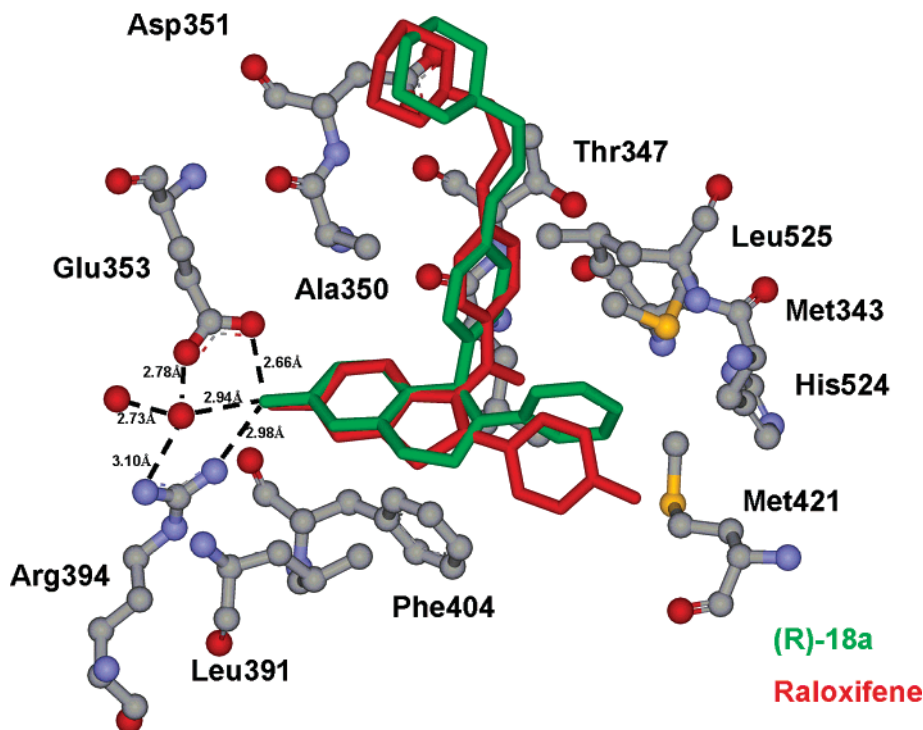


Figure 3. Superimposition of the X-ray crystal structures of (*R*)-**18a** (green) in complex with ER α -LBD_{301–553}/C \rightarrow S triple mutant and of raloxifene (**5**) in complex with ER α -LBD_{301–553}/carboxymethylated C. For details on the structure determination, see Supporting Information.

was readily purified to homogeneity by a three-step chromatography, and well-diffracting crystals were obtained. Noteworthy, the yield of the purified ER α -LBD mutant complex was 7-fold higher than that obtained with the wild-type protein (18.4 mg and 2.5 mg per liter of culture, respectively). The structure of the complex was solved to 2.28 Å. The final refined model includes residues 307–525 and 535–546 since the electron density for residues 301–306, 526–534, and 547–553 is not well resolved. The electron density of the ligand is well defined and reveals that only one enantiomer, that possessing the *R* absolute configuration, binds to ER α . The observation that one enantiomer has a significantly higher binding affinity than the other has been reported for SERMs such as lasofoxifene (**6**),¹⁴ NNC 45-0781, a *cis*-diaryl-hydroxychromane derivative,^{28a} and EM-652.^{28b} In the case of lasofoxifene (**6**),¹⁴ the absolute configuration of the most potent enantiomer was determined to correspond to the 1*R*,2*S* isomer as illustrated in Figure 1. Likewise, the pure enantiomer NNC 45-0781^{28a} was shown to possess a lasofoxifene-like absolute configuration. In a manner analogous to lasofoxifene (**6**) and NNC 45-0781, (*R*)-**18a** possesses an absolute configuration at C-1 which is estradiol-like. Thus, it appears reasonable that one enantiomer of racemic **18a** is more potent than the other and that the most active component of the racemate corresponds to the enantiomer which cocrystallized with the ER α -LBD mutant, that possessing the *R* absolute configuration.

An overlay of the X-ray crystal structures of the complexes of ER α -ligand binding domain (LBD) with (*R*)-**18a** and raloxifene (**5**) shows that both compounds bind to the same cleft of the receptor and display similarities in their binding modes (Figure 3). In both structures, the phenolic hydroxyl interacts with Glu353, Arg394, and a water molecule while the piperidine

nitrogen forms a salt-bridge with Asp351. The basic side chains of (*R*)-**18a** and raloxifene (**5**) adopt similar positions, thus placing the C-terminal helix (H-12, residues 536–544) into what has been described as the “antagonist” position.²⁵ The main difference between the two lies in the conformation of their “D ring” phenyl groups, that of **18a** being oriented almost perpendicularly to the plane of its tetrahydroisoquinolinol core while that of raloxifene (**5**) is tilted by $\sim 45^\circ$ out of planarity relative to its benzothiophene central core. In addition, since raloxifene’s phenyl ring bears a 4-OH group, it forms an additional hydrogen bond with His524, an interaction which cannot occur with **18a**.

Modeling Studies. On the basis of this information, it is possible that the *R* enantiomer of **20a** binds within ER α in an orientation similar to that observed for (*R*)-**18a** such that the methyl occupies the α -position. We used docking and modeling studies to confirm whether this could be the case. GOLD docking studies were initially performed using both enantiomers of **18a** and the X-ray crystal structure of raloxifene (**5**)²⁵ (See Supporting Information). The predicted binding mode of (*R*)-**18a** within the LBD of ER α was in agreement with the X-ray crystal structure of the ER α -LBD_{301–553}/C \rightarrow S triple mutant/(*R*)-**18a** complex. The same GOLD docking was repeated with each of the enantiomers of **20a**. As a result of this study, the *R* enantiomer of **20a** obtained a significantly better GOLD score than its mirror image and was predicted to adopt a binding mode similar to that of **18a**. We were therefore confident to use the X-ray crystal structure of the ER α -LBD mutant/(*R*)-**18a** complex to build a refined model of the complex of ER α -LBD mutant with (*R*)-**20a** by simply changing the C-1 hydrogen of (*R*)-**18a** by a methyl group, followed by a minimization protocol (See Supporting Information). The final model is illustrated in Figure 4. It indeed

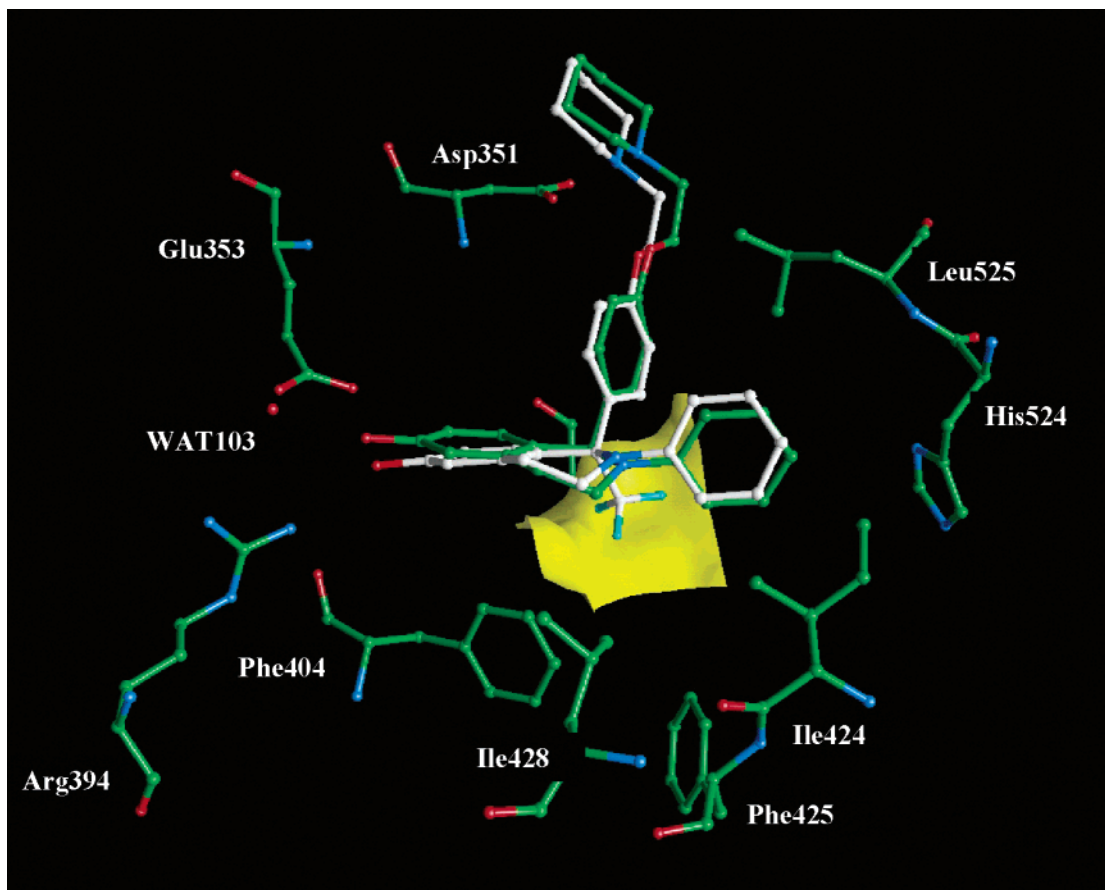


Figure 4. Model of (*R*)-**20a** (C atoms in white) binding to ER α -LBD₃₀₁₋₅₅₃/C \rightarrow S triple mutant compared to (*R*)-**18a** (X-ray structure, C atoms in green). For details on the docking and modeling studies, see Supporting Information. Only water WAT103 and amino acids Phe404, Arg394, Glu353, Asp351, Leu525, His524, Ile424, Phe425, Ile428 of ER α -LBD (X-ray structure with (*R*)-**18a**) are shown. The solvent accessible surface (in yellow) of the modeled receptor around the C-1 methyl group of **20a** is mainly formed by Leu346 which is hidden under the surface. This picture shows that the C-1 methyl group of (*R*)-**20a** is nicely accommodated in the model.

suggests that (*R*)-**20a** adopts a binding mode analogous to that of (*R*)-**18a**.

Conclusion

We have disclosed herein the outcome of our initial efforts to identify estrogen receptor modulators able to display mixed agonist/antagonist behaviors. More specifically, we have reported the discovery of tetrahydroisoquinolines which bind to the estrogen receptors with high affinity. We have shown that modification of the substitution pattern of the *N*-phenyl ring has a modest impact on potency in most instances but influences significantly the selectivity in the case of analogues bearing a *p*-*i*-Pr group. The pyrrolidine and piperidine derivatives **19e** and **20e** were found to exhibit up to 50-fold specificities for ER α over ER β . We have shown that addition of an aminoethoxy side chain and replacement of the 1-H in our initial lead **27** by a 1-Me furnished the potent ligand **20a**. This compound, along with a number of tetrahydroisoquinoline derivatives, displayed antagonistic properties in the MCF-7 assay, by inhibiting the proliferative action of 17 β -estradiol (**1**) on MCF-7 human breast cancer cells. The pharmacokinetic behavior of the tetrahydroisoquinolines could be attuned by means of appropriate substituents on the *N*-phenyl group. On the basis of their *in vitro* data and their promising pharmacokinetic properties, the *p*-F deriva-

tives **19c** and **20c** qualify as the most interesting candidates for further investigations. It remains to be determined whether such substances would have improved profiles *in vivo*.

The quest for the "ideal" SERM will certainly remain a challenge due to the fact that relatively minor structural changes greatly impact various tissue-specific effects that, in many cases, can only be assessed in animal models or in the clinic.

Experimental Section

Chemistry. General. All commercial chemicals and solvents are reagent grade and were used without further purification unless otherwise stated. Grignard reagents were obtained from commercial sources. All reactions except those in aqueous media were carried out under an atmosphere of N₂, in flame-dried glassware. Reactions were monitored by analytical reverse-phase high-pressure liquid chromatography (RP-HPLC) using a Hewlett-Packard Series 1100, equipped with a diode array spectrometer ($\lambda = 210-250$ nm) and a Waters Symmetry C-8 column (3.5 μ m, 2.1 \times 50 mm) as the stationary phase. The mobile phases used were A: 95:5 H₂O:CH₃CN containing 0.1% TFA and B: CH₃CN containing 0.1% TFA. The program employed ran as follows: 0 to 7 min: 5% B \rightarrow 100% B; 7 to 8.5 min: 100% B; At 8.5 min, 5% B for 2.5 min, prior to the next run. The flow rate was maintained at 0.5 mL/min. Additionally, thin-layer chromatography on 0.25 mm silica gel plates (E. Merck, silica gel 60 F₂₅₄) was used to follow the reactions. Visualization was accomplished with UV light, KMnO₄ or 5% phosphomolybdic acid in 95% ethanol.

Intermediates and final compounds were purified by flash chromatography (E. Merck silica gel 60, 230–400 mesh), crystallization, and/or semipreparative reverse-phase HPLC (RP-HPLC) using a Gilson model 306 equipped with a UV/Vis detector (λ usually set to 214 nm) and a Symmetry Prep RP18 (7 μ m, 19 \times 150 mm column) as the stationary phase. The eluents employed were A: H₂O containing 0.1% TFA and B: CH₃CN containing 0.1% TFA. The program ran as follows: 0–0.5 min, 100% B; 0.5–3 min, 10% B; the compound was automatically injected at 3 min; from 3 to 4 min, 10% B; a linear gradient was then run from 10% B to 100% B over the next 16 min followed by a 2.0 min hold at 100% B. The flow rate was held constant at 20 mL/min.

NMR spectra were recorded either on a Varian spectrometer, model Mercury-300 or -400 or on a Bruker DPX-400 or DMX-500 or DRX-500. Signal positions (δ values) were calibrated using the residual undeuterated solvent resonance as the internal standard. Coupling constants (J values) are given in hertz (Hz). The multiplicity is indicated by one of the following: d, doublet; t, triplet; m, multiplet; br, broad. Infrared spectra were recorded using a Perkin-Elmer *i*-Series FT-IR microscope coupled with a SPECTRUM 2000 FT-IR spectrometer. High-resolution mass spectra (HRMS) were recorded on a Finnigan MAT900.

N-Arylation Reactions. 6-Methoxy-3,4-dihydro-2*H*-isoquinolin-1-one (**22**) was N-arylated by reaction with an aryl iodide or an aryl bromide (2 equiv) in the presence of CuI (0.1 equiv to start with; portions of 0.1 equiv were then added, for a maximal amount of 0.4 equiv, in cases where the reaction was slowing down) and K₂CO₃ (1 equiv) in DMF (0.5–0.6 M) at 150 °C for 18.5–164 h. The yields of the arylated products varied between 48% and 95%, and most reactions were high yielding. A representative procedure is given below.

Synthesis of 6-Methoxy-2-(3-methoxyphenyl)-3,4-dihydro-2*H*-isoquinolin-1-one (23f**).** A mixture of 6-methoxy-3,4-dihydro-2*H*-isoquinolin-1-one (**22**, 7.2 g, 40.6 mmol), 3-bromoanisole (98%, 10.5 mL, 81.3 mmol), K₂CO₃ (99%, 5.67 g, 40.6 mmol), and CuI (0.774 g, 4.06 mmol) in DMF (70 mL) was heated at 150 °C for 30 h under N₂ atmosphere. After that period of time, a second portion of CuI (0.774 g, 4.06 mmol) was added. Heating was continued for another 40 h prior to the addition of a last portion of CuI (0.774 g, 4.06 mmol). After heating for a further 48 h, for a total reaction time of 118 h, the mixture was poured into aq NH₄OH (300 mL)/AcOEt (300 mL). The layers were separated, and the aqueous layer was extracted with portions of AcOEt (3 \times 300 mL). The combined organic phases were washed with brine (500 mL), dried over MgSO₄, and concentrated in vacuo until crystallization started. Hexane was added slowly to the solution. The resulting solid was filtered, washed with hexane, and dried in vacuo to provide the title compound (10.96 g, 95%): IR (KBr) ν_{max} : 1653, 1597, 1472, 1403, 1327, 1312, 1295, 1262, 1214, 1194, 1172, 1157, 1034, 1022, 851 cm⁻¹. ¹H NMR (500 MHz, CDCl₃) δ : 8.10 (d, J = 8.5 Hz, 1H), 7.30 (t, J = 8.0 Hz, 1H), 6.98–6.94 (m, 2H), 6.88 (dd, J = 2.5, 8.5 Hz, 1H), 6.80 (dm, J for d = 8.0 Hz, 1H), 6.72 (d, J = 2.5 Hz, 1H), 3.96 (t, J = 6.5 Hz, 2H), 3.88 (s, 3H), 3.83 (s, 3H), 3.10 (t, J = 6.5 Hz, 2H). ¹³C NMR (125.8 MHz, CDCl₃) δ : 163.8, 162.1, 159.5, 144.0, 140.0, 130.6, 129.1, 122.1, 117.0, 112.3, 111.6, 111.5, 110.9, 55.05, 55.0, 49.0, 28.6. HRMS (ESI, M + H⁺) calcd for C₁₇H₁₇NO₃: 284.1287; found: 284.1285. HPLC Purity: 98%; t_R 5.43 min.

Conversion of Lactams **23a–j into 1-Methyl-Tetrahydroisoquinolines **24a–j**.** Lactam **23(a–j)** was allowed to undergo reaction with 4-benzyloxyphenyllithium (1.1–1.5 equiv) in THF (0.12–0.14 M) for 0.75–3 h. 4-Benzyloxyphenyllithium was generated from 4-benzyloxyphenyl iodide or bromide (1.1–1.5 equiv) and *n*-BuLi in hexanes (1.1–1.5 equiv) at –78 °C in THF, 0.75–2 h. After aq workup and isolation, the iminium salt was dissolved in THF (0.1–0.2 M) and treated with MeMgBr (3 M in Et₂O, 1.5–2 equiv) at 0 °C. The ice bath was removed, and the reaction mixture was allowed to warm to rt. After the mixture was stirred at this temperature for 0.75–3 h, the product was isolated and purified. Tetrahydroisoquinolines **24a–j** were obtained in yields ranging from 47 to 90%. A representative example is given below.

Synthesis of 1-(4-Benzyloxyphenyl)-6-methoxy-2-(3-methoxyphenyl)-1-methyl-1,2,3,4-tetrahydroisoquinoline (24f**).** To a cold (–78 °C) solution of 4-benzyloxybromobenzene (98%, 5.0 g, 18.62 mmol) in anhyd THF (50 mL) was added a solution of *n*-BuLi in hexanes (1.6 M, 12.5 mL, 20.0 mmol) over a period of 20 min. After the resultant suspension was stirred at this temperature for 45 min, a solution of lactam **23f** (4.058 g, 14.3 mmol) in anhyd THF (70 mL) was added over a period of 20 min. Stirring was continued for an additional 50 min. The mixture was poured onto H₂O (200 mL)/AcOEt (200 mL). HClO₄ (70%, 3.7 mL) was added, the mixture was stirred for 10 min, and the pH of the aqueous layer was brought to ~5 by addition of sat. aq NaHCO₃. The layers were separated, and the aqueous phase was washed with AcOEt (3 \times 150 mL). The combined organic layers were washed with brine (200 mL) and dried over MgSO₄, and the solution was concentrated in vacuo yielding an iminium salt which was used directly in the next step.

To a cold (0 °C) solution of the iminium intermediate in anhyd THF (90 mL) was added a solution of MeMgBr in Et₂O (3M, 7.5 mL, 22.5 mmol) over a period of 10 min. The resultant mixture was stirred at 0 °C for 5 min and was allowed to warm to rt. After the suspension was stirred for 1 h, it was poured into sat. aq NH₄Cl (200 mL). The aqueous layer was extracted with CH₂Cl₂ (3 \times 200 mL), and the combined organic phases were washed with brine (200 mL), dried (MgSO₄), and concentrated in vacuo. The resultant wax was recrystallized from AcOEt/hexane to provide the title compound **24f** (4.74 g, 71%) as a solid: IR (KBr) ν_{max} : 1600, 1576, 1504, 1484, 1455, 1241, 1222, 1171, 1162, 1044, 1031, 1019, 751, 698 cm⁻¹. ¹H NMR (500 MHz, CDCl₃) δ : 7.46–7.32 (m, 5H), 7.18 (d, J = 8.8 Hz, 2H), 6.99 (t, J = 8.0 Hz, 1H), 6.85 (dd, J = 8.8 Hz, 2H), 6.73 (d, J = 8.5 Hz, 1H), 6.65 (d, J = 2.5 Hz, 1H), 6.63 (dd, J = 2.5, 8.5 Hz, 1H), 6.50 (dd, J = 2.0, 8.0 Hz, 1H), 6.31 (dd, J = 2.0, 8.0 Hz, 1H), 6.08 (t, J = 2.0 Hz, 1H), 5.03 (s, 2H), 3.76 (s, 3H), 3.54–3.38 (m, 2H), 3.46 (s, 3H), 3.21 (ddd, J = 5.0, 10.0, 15.5 Hz, 1H), 2.91 (ddd, J = 3.5, 3.5, 15.5 Hz, 1H), 1.68 (s, 3H). ¹³C NMR (125.8 MHz, CDCl₃) δ : 158.5, 156.9, 156.8, 151.5, 141.6, 136.8, 136.7, 135.0, 129.8, 129.2, 128.2, 127.9, 127.6, 127.1, 117.1, 113.5, 112.2, 111.8, 110.7, 108.6, 69.5, 64.1, 54.8, 54.4, 45.8, 30.6, 22.7. HRMS (ESI, M + H⁺) calcd for C₃₁H₃₁NO₃: 466.2382; found: 466.2385.

Debenzylation of **24a–j.** A solution of 1-methyl-tetrahydroisoquinoline **24(a–j)** in CH₂Cl₂ (0.04–0.06 M) was treated with AlCl₃ (3 equiv) in the presence of Me₂NPh (10 equiv) at rt for 1–1.5 h. Workup and purification afforded **25a–j** in yields varying between 44 and 75%. A representative example is reported below.

Synthesis of 4-[6-Methoxy-2-(3-methoxyphenyl)-1-methyl-1,2,3,4-tetrahydroisoquinolin-1-yl]phenol (25f**).** A solution of compound **24f** (4.5 g, 9.67 mmol), AlCl₃ (99%, 3.91 g, 29.0 mmol) and Me₂NPh (11.77 g, 96.6 mmol) in CH₂Cl₂ (250 mL) was stirred at rt for 1 h. H₂O (75 mL) and CH₂Cl₂ (300 mL) were then added to the reaction mixture, and the pH was brought to 5 with aq NaHCO₃. The layers were separated. The aqueous layer was extracted with CH₂Cl₂ (250 mL) and then with AcOEt (3 \times 250 mL). The combined organic layers were washed with brine, dried (MgSO₄), and concentrated in vacuo. The resultant oil was purified by flash chromatography (silica gel, 6:1 \rightarrow 5:1 \rightarrow 4:1 hexanes:EtOAc) to provide the tetrahydroisoquinoline **25f** (2.384 g, 66%) as a solid: IR (KBr) ν_{max} : 3600–3120, 1611, 1595, 1585, 1513, 1501, 1464, 1282, 1259, 1247, 1220, 1194, 1159, 1116, 1041, 1028 cm⁻¹. ¹H NMR (500 MHz, CDCl₃) δ : 7.13 (d, J = 8.5 Hz, 2H), 6.99 (t, J = 8.0 Hz, 1H), 6.75–6.59 (m, 5H), 6.50 (dd, J = 2.0, 8.0 Hz, 1H), 6.32 (dd, J = 2.0, 8.0 Hz, 1H), 6.09 (dd, J = 2.0, 2.0 Hz, 1H), 4.75 (s, 1H), 3.78 (s, 3H), 3.52 (s, 3H), 3.56–3.37 (m, 2H), 3.21 (ddd, J = 5.0, 10.0, 15.5 Hz, 1H), 2.91 (ddd, J = 3.5, 3.5, 15.5 Hz, 1H), 1.67 (s, 3H). ¹³C NMR (125.8 MHz, CDCl₃) δ : 159.0, 157.3, 154.1, 152.0, 142.0, 137.3, 135.5, 130.3, 129.9, 128.4, 117.7, 114.6, 112.7, 112.3, 111.4, 109.0, 64.6, 55.3, 55.0, 46.3, 31.1,

23.2. HRMS (ESI, M + H⁺) calcd for C₂₄H₂₅NO₃: 376.1913; found: 376.1918. HPLC Purity: 96%; t_R 4.08 min.

Synthesis of 19a–j, 20a–j and 26a via Alkylation of Phenols 25a–j Followed by Demethylation. Phenols 25a–j were alkylated by treatment with NaH (3 equiv) and the appropriate alkylating agent (HCl salt, 1.2–1.3 equiv) in dioxane (0.043–0.092 M) or in dioxane-DMF (22:1 or 36:1) at 80 °C for 1–20 h. Isolation provided quantitative yields of the alkylated materials.

Demethylation was achieved by treatment with AlCl₃ (5.9–6 equiv) in CH₂Cl₂ (0.019–0.043 M) in the presence of EtSH (5 equiv) at rt for 0.5–2 h. Yields of purified products varied between 22 and 75%. Representative examples are described below.

Synthesis of 6-Methoxy-2-(3-methoxyphenyl)-1-methyl-1-[4-(2-pyrrolidin-1-yl-ethoxy)phenyl]-1,2,3,4-tetrahydroisoquinoline. To a stirred solution of phenol 25f (400 mg, 1.07 mmol) in anhydrous dioxane (10 mL) was added a portion of NaH (60% in oil, 64 mg, 1.60 mmol). After stirring the suspension at rt for 10 min, a mixture of 1-(2-chloroethyl)-pyrrolidine·HCl (98%, 221.9 mg, 1.28 mmol) and NaH (60% in oil, 64 mg, 1.60 mmol) in dioxane (10 mL) was added to the solution. The reaction mixture was heated to 80 °C for 17.5 h. The mixture was cooled to rt and was poured onto sat. aq NaHCO₃ (50 mL)/AcOEt (50 mL). The layers were separated. The aqueous layer was further extracted with AcOEt (3 × 50 mL), and the combined organic phases were washed with brine (75 mL), dried over MgSO₄, and concentrated in vacuo to provide a quantitative yield of the pyrrolidine derivative: IR (KBr) ν_{max}: 1607, 1595, 1586, 1500, 1465, 1281, 1259, 1238, 1228, 1184, 1166, 1157, 1067, 1040, 809 cm⁻¹. ¹H NMR (500 MHz, CDCl₃) δ: 7.16 (dm, *J* for *d* = 8.8 Hz, 2H), 6.98 (t, *J* = 8.0 Hz, 1H), 6.78 (dm, *J* for *d* = 8.8 Hz, 2H), 6.72 (d, *J* = 8.5 Hz, 1H), 6.64 (d, *J* = 2.5 Hz, 1H), 6.62 (dd, *J* = 2.5, 8.5 Hz, 1H), 6.49 (dd, *J* = 2.0, 8.0 Hz, 1H), 6.29 (dd, *J* = 2.0, 8.0 Hz, 1H), 6.10 (dd, *J* = 2.0, 2.0 Hz, 1H), 4.09 (t, *J* = 6.0 Hz, 2H), 3.78 (s, 3H), 3.51 (s, 3H), 3.54–3.38 (m, 2H), 3.21 (ddd, *J* = 5.0, 10.0, 15.0 Hz, 1H), 2.95–2.85 (m, 3H), 2.71–2.56 (m, 4H), 1.87–1.77 (m, 4H), 1.67 (s, 3H). ¹³C NMR (125.8 MHz, CDCl₃) δ: 158.5, 156.9, 156.7, 151.5, 141.4, 136.8, 135.0, 129.8, 129.1, 127.8, 117.2, 113.2, 112.2, 111.8, 110.8, 108.5, 66.4, 64.0, 54.8, 54.7, 54.4, 54.3, 45.8, 30.6, 23.1, 22.7. HRMS (ESI, M + H⁺) calcd for C₃₀H₃₆N₂O₃: 473.2804; found: 473.2801.

Synthesis of 2-(3-Hydroxyphenyl)-1-methyl-1-[4-(2-pyrrolidin-1-yl-ethoxy)phenyl]-1,2,3,4-tetrahydroisoquinolin-6-ol (19f). A mixture of the pyrrolidine derivative (50 mg, 0.106 mmol), AlCl₃ (84.1 mg, 0.624 mmol), and EtSH (97%, 40.3 μL, 0.529 mmol) in CH₂Cl₂ (5 mL) was stirred at room temperature for 30 min. The mixture was diluted with CH₂Cl₂ (50 mL), and H₂O (50 mL) was added. The pH was adjusted to ~6 with sat. aq NaHCO₃. The layers were separated, and the aqueous layer was washed with CH₂Cl₂ (3 × 50 mL). The combined organic phases were washed with brine (50 mL), dried (MgSO₄), and concentrated in vacuo. The gray-greenish residue was purified by reverse phase HPLC to provide the title compound as a white solid (18.1 mg, 39%): ¹H NMR (400 MHz, DMSO) δ: 9.17 (s, 1H), 9.15 (s, 1H), 7.12 (d, *J* = 8.8 Hz, 2H), 6.80–6.71 (m, 3H), 6.56 (d, *J* = 8.5 Hz, 1H), 6.48 (d, *J* = 2.0 Hz, 1H), 6.44 (dd, *J* = 2.0, 8.5 Hz, 1H), 6.27 (dd, *J* = 2.0, 8.0 Hz, 1H), 6.10 (br s, 1H), 5.94 (dd, *J* = 2.0, 8.0 Hz, 1H), 4.00 (t, *J* = 6.0 Hz, 2H), 3.40–3.20 (m, 3H), 3.07–2.97 (m, 1H), 2.76 (t, *J* = 6.0 Hz, 2H), 2.57–2.46 (m, 4H), 1.72–1.63 (m, 4H), 1.67 (s, 3H). HRMS (ESI, M + H⁺) calcd for C₂₈H₃₂N₂O₃: 445.2491; found: 445.2592. HPLC Purity: 100%; t_R 3.32 min.

Synthesis of 6-Methoxy-2-(3-methoxyphenyl)-1-methyl-1-[4-(2-piperidin-1-yl-ethoxy)phenyl]-1,2,3,4-tetrahydroisoquinoline. To a stirred solution of phenol 25f (400 mg, 1.07 mmol) in anhydrous dioxane (10 mL) was added a portion of NaH (60% in oil, 64 mg, 1.60 mmol). After stirring the suspension at rt for 10 min, a mixture of 1-(2-chloroethyl)-piperidine·HCl (97%, 242.7 mg, 1.28 mmol) and NaH (60% in oil, 64 mg, 1.60 mmol) in dioxane (10 mL) was added to the reaction mixture. The suspension was heated to 80 °C for 5 h. The mixture was then cooled to rt and was poured onto sat.

aq NaHCO₃ (50 mL)/AcOEt (50 mL). The layers were separated, and the aqueous layer was further extracted with AcOEt (3 × 50 mL). The combined organic phases were washed with brine (75 mL), dried over MgSO₄, and concentrated in vacuo to provide a quantitative yield of the piperidine derivative: IR (KBr) ν_{max}: 2932, 1600, 1576, 1500, 1485, 1467, 1455, 1306, 1244, 1222, 1164, 1116, 1037, 839 cm⁻¹. ¹H NMR (500 MHz, CDCl₃) δ: 7.16 (dm, *J* for *d* = 8.8 Hz, 2H), 6.98 (t, *J* = 8.0 Hz, 1H), 6.76 (dm, *J* for *d* = 8.8 Hz, 2H), 6.72 (d, *J* = 8.5 Hz, 1H), 6.64 (d, *J* = 2.5 Hz, 1H), 6.62 (dd, *J* = 2.5, 8.5 Hz, 1H), 6.49 (dd, *J* = 2.0, 8.0 Hz, 1H), 6.29 (dd, *J* = 2.0, 8.0 Hz, 1H), 6.09 (dd, *J* = 2.0, 2.0 Hz, 1H), 4.08 (br t, *J* = 5.5 Hz, 2H), 3.77 (s, 3H), 3.50 (s, 3H), 3.54–3.37 (m, 2H), 3.21 (ddd, *J* = 5.0, 10.0, 15.5 Hz, 1H), 2.91 (ddd, *J* = 3.5, 3.5, 15.5 Hz, 1H), 2.82–2.73 (m, 2H), 2.59–2.40 (m, 4H), 1.67 (s, 3H), 1.65–1.55 (m, 4H), 1.49–1.39 (m, 2H). ¹³C NMR (125.8 MHz, CDCl₃) δ: 159.05, 157.4, 157.3, 152.0, 141.9, 137.3, 135.5, 130.3, 129.6, 128.4, 117.7, 113.7, 112.7, 112.3, 111.3, 109.0, 65.9, 64.6, 58.1, 55.3, 55.2, 54.9, 46.3, 31.1, 26.0, 24.3, 23.2. HRMS (ESI, M + H⁺) calcd for C₃₁H₃₈N₂O₃: 487.2961; found: 487.2963.

Synthesis of 2-(3-Hydroxyphenyl)-1-methyl-1-[4-(2-piperidin-1-yl-ethoxy)phenyl]-1,2,3,4-tetrahydroisoquinoline (20f). A mixture of piperidine derivative (518.4 mg, 1.065 mmol), AlCl₃ (99%, 846.5 mg, 6.28 mmol), and EtSH (97%, 406 μL, 5.33 mmol) in CH₂Cl₂ (25 mL) was stirred at rt for 1.5 h. The mixture was diluted with CH₂Cl₂ (50 mL), and H₂O (50 mL) was added. The pH was adjusted to ~5–6 with sat. aq NaHCO₃. The layers were separated, and the aqueous layer was extracted with CH₂Cl₂ (3 × 50 mL). The combined organic phases were washed with brine (50 mL), dried (MgSO₄), and concentrated in vacuo. The gray-greenish residue was purified by reverse phase HPLC to provide the title compound as a white solid (181.6 mg, 37%): IR (KBr) ν_{max}: 3650–2200, 2932, 1606, 1589, 1239, 1182, 1130, 1035, 849, 829, 770 cm⁻¹. ¹H NMR (400 MHz, DMSO) δ: 9.12 (s, 1H), 8.93 (s, 1H), 7.12 (d, *J* = 8.8 Hz, 2H), 6.82–6.70 (m, 3H), 6.58 (d, *J* = 8.5 Hz, 1H), 6.49 (d, *J* = 2.5 Hz, 1H), 6.45 (dd, *J* = 2.5, 8.5 Hz, 1H), 6.28 (dd, *J* = 2.0, 8.0 Hz, 1H), 6.12 (t, *J* = 2.0 Hz, 1H), 5.97 (dd, *J* = 2.0, 8.0 Hz, 1H), 4.02 (t, *J* = 6.0 Hz, 2H), 3.40–3.20 (m, 2H), 3.08–2.95 (m, 1H), 2.78 (dm, *J* for *d* = 16.0 Hz, 1H), 2.73–2.61 (m, 2H), 2.53–2.37 (m, 4H), 1.61 (s, 3H), 1.57–1.45 (m, 4H), 1.44–1.32 (m, 2H). ¹³C NMR (100.6 MHz, DMSO) δ: 156.8, 156.5, 154.6, 151.6, 141.8, 135.1, 134.8, 129.5, 128.6, 127.9, 115.3, 113.7, 113.6, 113.4, 111.4, 109.0, 65.1, 63.6, 57.3, 54.3, 45.8, 30.2, 25.3, 23.7, 23.2. HRMS (ESI, M + H⁺) calcd for C₂₉H₃₄N₂O₃: 459.2648; found: 459.2652. HPLC Purity: 100%; t_R 3.38 min.

2-Phenyl-1-[4-(2-pyrrolidin-1-yl-ethoxy)phenyl]-1,2,3,4-tetrahydroisoquinolin-6-ol (17a). IR (KBr) ν_{max}: 3650–2200, 3023, 2953, 2816, 1597, 1504, 1381, 1326, 1289, 1244, 1169, 1035, 860, 748, 692 cm⁻¹. ¹H NMR (400 MHz, DMSO) δ: 9.35 (br s, 1H), 7.23–7.10 (m, 5H), 6.88–6.78 (m, 4H), 6.70–6.58 (m, 3H), 5.80 (s, 1H), 4.01 (t, *J* = 6.0 Hz, 2H), 3.70–3.60 (m, 1H), 3.46–3.26 (m, 1H), 2.94–2.74 (m, 4H), 2.62–2.48 (m, 4H), 1.74–1.63 (m, 4H). ¹³C NMR (125.8 MHz, DMSO) δ: 157.4, 156.4, 149.3, 136.5, 136.4, 129.3, 129.1, 128.9, 128.3, 116.9, 114.6, 114.3, 113.53, 113.48, 66.7, 60.7, 54.6, 54.3, 43.3, 27.9, 23.4. HRMS (ESI, M + H⁺) calcd for C₂₇H₃₀N₂O₂: 415.2386; found: 415.2387. HPLC Purity: 98%; t_R 3.71 min.

2-Phenyl-1-[4-(2-piperidin-1-yl-ethoxy)phenyl]-1,2,3,4-tetrahydroisoquinolin-6-ol (18a). IR (KBr) ν_{max}: 3600–2200, 2939, 1608, 1594, 1504, 1480, 1380, 1245, 746, 690 cm⁻¹. ¹H NMR (400 MHz, DMSO) δ: 9.31 (s, 1H), 7.21–7.10 (m, 5H), 6.82 (d, *J* = 8.5 Hz, 4H), 6.70–6.58 (m, 3H), 5.79 (s, 1H), 3.99 (t, *J* = 6.0 Hz, 2H), 3.70–3.60 (m, 1H), 3.44–3.29 (m, 1H), 2.93–2.74 (m, 2H), 2.62 (t, *J* = 6.0 Hz, 2H), 2.47–2.35 (m, 4H), 1.55–1.43 (m, 4H), 1.41–1.32 (m, 2H). ¹³C NMR (125.8 MHz, DMSO) δ: 157.1, 156.0, 149.0, 136.2, 136.0, 129.0, 128.8, 128.6, 128.0, 116.6, 114.3, 114.0, 113.2, 113.1, 65.4, 60.3, 57.4, 54.4, 42.9, 27.5, 25.5, 23.9. HRMS (ESI, M + H⁺) calcd for C₂₈H₃₂N₂O₂: 429.2542; found: 429.2540. HPLC Purity: 98%; t_R 3.86 min.

1-Methyl-2-phenyl-1-[4-(2-pyrrolidin-1-yl-ethoxy)phenyl]-1,2,3,4-tetrahydroisoquinolin-6-ol (19a). IR (KBr)

ν_{\max} : 3650–2000, 2906, 2804, 1606, 1506, 1490, 1240, 1227, 1183, 847, 839, 765 cm^{-1} . $^1\text{H NMR}$ (500 MHz, DMSO) δ : 9.22 (s, 1H), 7.14 (d, $J = 8.8$ Hz, 2H), 7.04 (t, $J = 7.5$ Hz, 2H), 6.87 (t, $J = 7.5$ Hz, 1H), 6.80 (d, $J = 8.8$ Hz, 2H), 6.60 (d, $J = 7.5$ Hz, 2H), 6.57 (d, $J = 8.5$ Hz, 1H), 6.53 (d, $J = 2.5$ Hz, 1H), 6.47 (dd, $J = 2.5, 8.5$ Hz, 1H), 4.04 (t, $J = 6.0$ Hz, 2H), 3.50–3.30 (m, 2H), 3.13–3.03 (m, 1H), 2.86–2.76 (m, 3H), 2.61–2.50 (m, 4H), 1.76–1.67 (m, 4H), 1.60 (s, 3H). $^{13}\text{C NMR}$ (125.8 MHz, DMSO) δ : 156.9, 154.9, 150.5, 141.8, 135.3, 135.1, 129.9, 129.1, 127.9, 124.6, 122.3, 113.9, 113.8, 113.6, 66.5, 64.0, 54.5, 54.2, 45.9, 30.6, 23.3, 23.1. HRMS (ESI, $\text{M} + \text{H}^+$) calcd for $\text{C}_{28}\text{H}_{32}\text{N}_2\text{O}_2$: 429.2542; found: 429.2538. HPLC Purity: 98%; t_{R} 3.37 min.

1-Methyl-2-phenyl-1-[4-(2-piperidin-1-yl-ethoxy)phenyl]-1,2,3,4-tetrahydroisoquinolin-6-ol (20a). IR (KBr) ν_{\max} : 3650–2300, 2937, 1609, 1593, 1508, 1491, 1238, 1228, 1183, 837, 767 cm^{-1} . $^1\text{H NMR}$ (500 MHz, DMSO) δ : 8.78 (s, 1H), 7.13 (d, $J = 8.8$ Hz, 2H), 7.04 (t, $J = 7.5$ Hz, 2H), 6.87 (t, $J = 7.5$ Hz, 1H), 6.79 (d, $J = 8.8$ Hz, 2H), 6.68 (d, $J = 7.5$ Hz, 2H), 6.64 (d, $J = 8.5$ Hz, 1H), 6.55 (d, $J = 2.5$ Hz, 1H), 6.50 (dd, $J = 2.5, 8.5$ Hz, 1H), 4.10 (t, $J = 5.5$ Hz, 2H), 3.48–3.38 (m, 2H), 3.07–2.93 (m, 1H), 2.90–2.75 (m, 3H), 2.68–2.54 (m, 4H), 1.67 (s, 3H), 1.64–1.53 (m, 4H), 1.50–1.42 (m, 2H). $^{13}\text{C NMR}$ (125.8 MHz, DMSO, 80 °C) δ : 157.3, 155.3, 150.8, 142.1, 135.63, 135.56, 129.7, 129.3, 128.0, 125.1, 122.4, 114.5, 114.3, 114.2, 66.0, 64.1, 57.5, 54.6, 46.6, 30.6, 25.5, 24.4, 23.9. HRMS (ESI, $\text{M} + \text{H}^+$) calcd for $\text{C}_{29}\text{H}_{34}\text{N}_2\text{O}_2$: 443.2699; found: 443.2698. HPLC Purity: 100%; t_{R} 3.52 min.

1-[4-(2-Azepan-1-yl-ethoxy)phenyl]-1-methyl-2-phenyl-1,2,3,4-tetrahydroisoquinolin-6-ol (26a). IR (KBr) ν_{\max} : 2924, 2853, 1609, 1509, 1490, 1361, 1331, 1249, 1227, 1185, 831, 703 cm^{-1} . $^1\text{H NMR}$ (500 MHz, DMSO) δ : 10.22 (br s, 1H), 9.22 (s, 1H), 7.19 (d, $J = 8.8$ Hz, 2H), 7.05 (t, $J = 8.0$ Hz, 2H), 6.92–6.84 (m, 3H), 6.61 (d, $J = 8.0$ Hz, 2H), 6.58 (d, $J = 8.5$ Hz, 1H), 6.53 (d, $J = 2.5$ Hz, 1H), 6.48 (dd, $J = 2.5, 8.5$ Hz, 1H), 4.43–4.26 (br s, 2H), 3.60–3.17 (m, 8H), 3.14–3.02 (m, 1H), 2.90–2.77 (m, 2H), 1.93–1.77 (m, 4H), 1.74–1.53 (m, 7H). $^{13}\text{C NMR}$ (125.8 MHz, DMSO) δ : 156.3, 155.2, 150.7, 142.9, 135.4, 135.3, 130.1, 129.4, 128.1, 124.8, 122.5, 114.2, 114.1, 114.1, 65.3, 64.2, 55.4, 54.8, 46.2, 30.7, 26.5, 23.5, 23.2. HRMS (ESI, $\text{M} + \text{H}^+$) calcd for $\text{C}_{30}\text{H}_{36}\text{N}_2\text{O}_2$: 457.2850; found: 457.2850. HPLC Purity: 98%; t_{R} 3.36 min.

1-Methyl-1-[4-(2-pyrrolidin-1-yl-ethoxy)phenyl]-2-*p*-tolyl-1,2,3,4-tetrahydroisoquinolin-6-ol (19b). IR (KBr) ν_{\max} : 3650–2200, 2958, 2929, 2825, 1511, 1499, 1478, 1295, 1247, 1199, 1181, 1034, 850, 822, 804 cm^{-1} . $^1\text{H NMR}$ (300 MHz, CD_3OD) δ : 7.06 (d, $J = 8.8$ Hz, 2H), 6.82 (d, $J = 8.0$ Hz, 2H), 6.79 (d, $J = 8.8$ Hz, 2H), 6.63–6.43 (m, 5H), 4.10 (t, $J = 5.5$ Hz, 2H), 3.46–3.36 (m, 1H), 3.33–3.26 (m, 1H), 3.13–3.00 (m, 1H), 2.97 (t, $J = 5.5$ Hz, 2H), 2.85 (ddd, $J = 4.5, 4.5, 16.0$ Hz, 1H), 2.80–2.67 (m, 4H), 2.19 (s, 3H), 1.93–1.77 (m, 4H), 1.62 (s, 3H). HRMS (ESI, $\text{M} + \text{H}^+$) calcd for $\text{C}_{29}\text{H}_{34}\text{N}_2\text{O}_2$: 443.2699; found: 443.2699. HPLC Purity: 98%; t_{R} 3.47 min.

1-Methyl-1-[4-(2-piperidin-1-yl-ethoxy)phenyl]-2-*p*-tolyl-1,2,3,4-tetrahydroisoquinolin-6-ol (20b). IR (KBr) ν_{\max} : 3650–2200, 2969, 2938, 2817, 1610, 1507, 1465, 1302, 1238, 1225, 1185, 1134, 839 cm^{-1} . $^1\text{H NMR}$ (400 MHz, DMSO) δ : 9.18 (s, 1H), 7.07 (d, $J = 8.8$ Hz, 2H), 6.82 (d, $J = 8.0$ Hz, 2H), 6.76 (d, $J = 8.8$ Hz, 2H), 6.55–6.40 (m, 5H), 4.00 (t, $J = 6.0$ Hz, 2H), 3.43–3.25 (m, 1H), 3.25–3.17 (m, 1H), 3.08–2.95 (m, 1H), 2.76 (dm, J for $d = 16.0$ Hz, 1H), 2.62 (t, $J = 6.0$ Hz, 2H), 2.47–2.34 (m, 4H), 2.14 (s, 3H), 1.53 (s, 3H), 1.53–1.43 (m, 4H), 1.40–1.30 (m, 2H). $^{13}\text{C NMR}$ (125.8 MHz, DMSO) δ : 156.8, 154.7, 147.8, 141.5, 135.2, 134.9, 131.4, 129.8, 129.2, 128.2, 125.1, 113.7, 113.6, 113.3, 65.3, 63.7, 57.5, 54.5, 45.9, 30.4, 25.6, 23.9, 22.8, 20.3. HRMS (ESI, $\text{M} + \text{H}^+$) calcd for $\text{C}_{30}\text{H}_{36}\text{N}_2\text{O}_2$: 457.2855; found: 457.2855. HPLC Purity: 100%; t_{R} 3.59 min.

2-(4-Fluorophenyl)-1-methyl-1-[4-(2-pyrrolidin-1-yl-ethoxy)phenyl]-1,2,3,4-tetrahydroisoquinolin-6-ol (19c). IR (KBr) ν_{\max} : 3650–2000, 2920, 2837, 1607, 1505, 1237, 1220, 841 cm^{-1} . $^1\text{H NMR}$ (500 MHz, DMSO) δ : 9.23 (s, 1H), 7.09 (d, $J = 8.8$ Hz, 2H), 6.89 (t, $J = 9.0$ Hz, 2H), 6.80 (d, $J = 8.8$ Hz, 2H), 6.65–6.56 (m, 2H), 6.55 (d, $J = 8.5$ Hz, 1H), 6.53 (d, $J =$

2.5 Hz, 1H), 6.47 (dd, $J = 2.5, 8.5$ Hz, 1H), 4.03 (t, $J = 6.0$ Hz, 2H), 3.48–3.38 (m, 1H), 3.28–3.18 (m, 1H), 3.11–3.00 (m, 1H), 2.85–2.74 (m, 3H), 2.58–2.46 (m, 4H), 1.77–1.64 (m, 4H), 1.56 (s, 3H). $^{13}\text{C NMR}$ (125.8 MHz, DMSO) δ : 158.3 (d, $J_{\text{C-F}} = 239$ Hz), 157.0, 155.0, 146.8, 141.2, 135.1, 135.0, 130.0, 129.4, 127.1 (d, $J_{\text{C-F}} = 8$ Hz), 114.35 (d, $J_{\text{C-F}} = 22$ Hz), 113.9, 113.8, 113.5, 66.7, 63.95, 54.6, 54.25, 46.2, 30.5, 23.3, 22.95. HRMS (ESI, $\text{M} + \text{H}^+$) calcd for $\text{C}_{28}\text{H}_{31}\text{FN}_2\text{O}_2$: 447.2448; found: 447.2446. HPLC Purity: 100%; t_{R} 3.49 min.

2-(4-Fluorophenyl)-1-methyl-1-[4-(2-piperidin-1-yl-ethoxy)phenyl]-1,2,3,4-tetrahydroisoquinolin-6-ol (20c). IR (KBr) ν_{\max} : 3650–2300, 2936, 1610, 1501, 1240, 1229, 1206, 1195, 1183, 839 cm^{-1} . $^1\text{H NMR}$ (500 MHz, DMSO) δ : 9.19 (s, 1H), 7.06 (d, $J = 8.5$ Hz, 2H), 6.87 (t, $J = 8.7$ Hz, 2H), 6.77 (d, $J = 8.5$ Hz, 2H), 6.59–6.54 (m, 2H), 6.52 (d, $J = 8.5$ Hz, 1H), 6.50 (d, $J = 2.0$ Hz, 1H), 6.44 (dd, $J = 2.0, 8.5$ Hz, 1H), 3.99 (t, $J = 6.0$ Hz, 2H), 3.45–3.37 (m, 1H), 3.25–3.17 (m, 1H), 3.08–3.00 (m, 1H), 2.77 (dm, J for $d = 16.0$ Hz, 1H), 2.62 (t, $J = 6.0$ Hz, 2H), 2.41 (br s, 4H), 1.54 (s, 3H), 1.53–1.45 (m, 4H), 1.42–1.33 (m, 2H). $^{13}\text{C NMR}$ (125.8 MHz, DMSO) δ : 158.1 (d, $J_{\text{C-F}} = 239$ Hz), 156.9, 154.8, 146.7, 141.0, 134.9, 134.8, 129.8, 129.2, 127.0 (d, $J_{\text{C-F}} = 8$ Hz), 114.2 (d, $J_{\text{C-F}} = 22$ Hz), 113.7, 113.6, 113.4, 65.4, 63.8, 57.5, 54.5, 46.0, 30.3, 25.6, 24.0, 22.8. HRMS (ESI, $\text{M} + \text{H}^+$) calcd for $\text{C}_{29}\text{H}_{33}\text{FN}_2\text{O}_2$: 461.2604; found: 461.2606. HPLC Purity: 99%; t_{R} 3.72 min.

2-(4-Chlorophenyl)-1-methyl-1-[4-(2-pyrrolidin-1-yl-ethoxy)phenyl]-1,2,3,4-tetrahydroisoquinolin-6-ol (19d). IR (KBr) ν_{\max} : 3650–2100, 2968, 2921, 2826, 1606, 1585, 1505, 1489, 1476, 1308, 1238, 1226, 1179, 1044, 836 cm^{-1} . $^1\text{H NMR}$ (500 MHz, DMSO) δ : 9.20 (s, 1H), 7.11 (d, $J = 8.5$ Hz, 2H), 7.05 (d, $J = 8.8$ Hz, 2H), 6.78 (d, $J = 8.5$ Hz, 2H), 6.60–6.50 (m, 3H), 6.49 (d, $J = 2.0$ Hz, 1H), 6.44 (dd, $J = 2.0, 8.5$ Hz, 1H), 4.00 (t, $J = 6.0$ Hz, 2H), 3.48–3.22 (m, 2H), 3.12–3.00 (m, 1H), 2.81–2.71 (m, 3H), 2.57–2.43 (m, 4H), 1.73–1.63 (m, 4H), 1.58 (s, 3H). $^{13}\text{C NMR}$ (125.8 MHz, DMSO) δ : 156.9, 154.8, 149.2, 141.1, 135.0, 134.8, 129.8, 129.0, 127.6, 125.9, 125.7, 113.75, 113.55, 66.5, 63.9, 54.4, 54.1, 45.7, 30.3, 23.2, 22.8. HRMS (ESI, $\text{M} + \text{H}^+$) calcd for $\text{C}_{28}\text{H}_{31}\text{ClN}_2\text{O}_2$: 463.2152; found: 463.2150. HPLC Purity: 96%; t_{R} 3.97 min.

2-(4-Chlorophenyl)-1-methyl-1-[4-(2-piperidin-1-yl-ethoxy)phenyl]-1,2,3,4-tetrahydroisoquinolin-6-ol (20d). IR (KBr) ν_{\max} : 3650–2100, 2941, 1606, 1585, 1503, 1488, 1477, 1302, 1238, 1226, 1179, 1049, 1039, 836 cm^{-1} . $^1\text{H NMR}$ (500 MHz, DMSO) δ : 9.21 (s, 1H), 7.11 (d, $J = 8.8$ Hz, 2H), 7.06 (d, $J = 8.8$ Hz, 2H), 6.79 (d, $J = 8.8$ Hz, 2H), 6.60–6.50 (m, 3H), 6.50 (d, $J = 2.5$ Hz, 1H), 6.44 (dd, $J = 2.5, 8.5$ Hz, 1H), 4.00 (t, $J = 6.0$ Hz, 2H), 3.46–3.22 (m, 2H), 3.12–3.00 (m, 1H), 2.78 (dm, $J = 16.0$ Hz, 1H), 2.64 (br s, 2H), 2.43 (s, 4H), 1.59 (s, 3H), 1.53–1.43 (m, 4H), 1.40–1.30 (m, 2H). $^{13}\text{C NMR}$ (125.8 MHz, DMSO) δ : 156.9, 154.8, 149.2, 141.1, 135.0, 134.7, 129.7, 128.9, 127.6, 125.9, 125.7, 113.7, 113.6, 65.3, 63.9, 57.45, 54.45, 45.7, 30.3, 25.5, 23.9, 22.8. HRMS (ESI, $\text{M} + \text{H}^+$) calcd for $\text{C}_{29}\text{H}_{33}\text{ClN}_2\text{O}_2$: 477.2309; found: 477.2305. HPLC Purity: 99%; t_{R} 4.11 min.

2-(4-Isopropylphenyl)-1-methyl-1-[4-(2-pyrrolidin-1-yl-ethoxy)phenyl]-1,2,3,4-tetrahydroisoquinolin-6-ol (19e). IR (KBr) ν_{\max} : 3650–2200, 2957, 2934, 2825, 1499, 1478, 1370, 1331, 1296, 1244, 1180, 1119, 1031, 851, 836 cm^{-1} . $^1\text{H NMR}$ (400 MHz, CDCl_3) δ : 7.05 (d, $J = 8.8$ Hz, 2H), 6.94 (d, $J = 8.5$ Hz, 2H), 6.69 (d, $J = 8.5$ Hz, 1H), 6.63 (d, $J = 8.8$ Hz, 2H), 6.60–6.48 (m, 4H), 4.12 (t, $J = 5.5$ Hz, 2H), 3.43–3.28 (m, 2H), 3.10–2.70 (m, 9H), 1.90 (br s, 4H), 1.67 (s, 3H), 1.205 (d, $J = 7.0$ Hz, 3H), 1.20 (d, $J = 7.0$ Hz, 3H). $^{13}\text{C NMR}$ (100.6 MHz, CDCl_3) δ : 157.0, 154.3, 148.1, 143.5, 141.5, 136.0, 135.9, 130.0, 129.5, 126.1, 125.6, 114.5, 113.8, 113.2, 66.0, 64.0, 55.2, 54.6, 46.4, 33.4, 30.5, 24.1, 24.0, 23.4. HRMS (ESI, $\text{M} + \text{H}^+$) calcd for $\text{C}_{31}\text{H}_{38}\text{N}_2\text{O}_2$: 471.3012; found: 471.3016. HPLC Purity: 99%; t_{R} 3.96 min.

2-(4-Isopropylphenyl)-1-methyl-1-[4-(2-piperidin-1-yl-ethoxy)phenyl]-1,2,3,4-tetrahydroisoquinolin-6-ol (20e). IR (KBr) ν_{\max} : 3700–2400, 2955, 2930, 1592, 1500, 1480, 1370, 1361, 1296, 1248, 1179, 1025, 851, 838 cm^{-1} . $^1\text{H NMR}$ (400 MHz, CDCl_3) δ : 7.06 (d, $J = 8.8$ Hz, 2H), 6.94 (d, $J = 8.5$ Hz, 2H), 6.70 (d, $J = 8.5$ Hz, 1H), 6.62 (d, $J = 8.8$ Hz, 2H), 6.60–

6.50 (m, 4H), 4.11 (t, $J = 6.0$ Hz, 2H), 3.44–3.28 (m, 2H), 3.07–2.96 (m, 1H), 2.93–2.75 (m, 4H), 2.72–2.53 (br s, 4H), 1.79–1.58 (m, 4H), 1.67 (s, 3H), 1.57–1.44 (m, 2H), 1.21 (d, $J = 7.0$ Hz, 3H), 1.20 (d, $J = 7.0$ Hz, 3H). ^{13}C NMR (100.6 MHz, CDCl_3) δ : 157.0, 154.0, 148.1, 143.5, 141.5, 136.3, 135.9, 130.1, 129.5, 126.1, 125.6, 114.4, 113.8, 113.2, 64.8, 64.1, 58.1, 55.0, 46.4, 33.4, 30.6, 25.3, 24.1, 24.0. HRMS (ESI, $\text{M} + \text{H}^+$) calcd for $\text{C}_{32}\text{H}_{40}\text{N}_2\text{O}_2$: 485.3168; found: 485.3166. HPLC Purity: 100%; t_{R} 4.05 min.

2-(3-Fluorophenyl)-1-methyl-1-[4-(2-pyrrolidin-1-yl-ethoxy)phenyl]-1,2,3,4-tetrahydroisoquinolin-6-ol (19g). IR (KBr) ν_{max} : 3650–2100, 3067, 3024, 2969, 2922, 2828, 1608, 1581, 1505, 1485, 1375, 1302, 1241, 1182, 1167, 1043, 900, 827, 779, 700 cm^{-1} . ^1H NMR (500 MHz, CD_3OD) δ : 7.15 (d, $J = 8.5$ Hz, 2H), 6.99 (dt, $J = 8.0, 8.0$ Hz, 1H), 6.81 (d, $J = 8.5$ Hz, 2H), 6.60 (d, $J = 8.5$ Hz, 1H), 6.62–6.53 (m, 2H), 6.50–6.44 (m, 2H), 6.25 (dm, J for $d = 12.5$ Hz, 1H), 4.11 (t, $J = 5.5$ Hz, 2H), 3.52–3.38 (m, 2H), 3.12 (ddd, $J = 5.0, 10.0, 16.0$ Hz, 1H), 2.91 (t, $J = 5.5$ Hz, 2H), 2.85 (ddd, $J = 4.0, 4.0, 16.0$ Hz, 1H), 2.72–2.62 (m, 4H), 1.87–1.78 (m, 4H), 1.68 (s, 3H). ^{13}C NMR (125.8 MHz, CDCl_3) δ : 163.8 (d, $J_{\text{C-F}} = 242$ Hz), 158.8, 156.1, 153.9 (d, $J_{\text{C-F}} = 9.5$ Hz), 142.9, 137.1, 136.5, 131.1, 130.5, 129.6 (d, $J_{\text{C-F}} = 9.5$ Hz), 121.5, 114.9, 114.7, 112.8 (d, $J_{\text{C-F}} = 22.5$ Hz), 109.7 (d, $J_{\text{C-F}} = 21.5$ Hz), 67.6, 65.7, 56.1, 55.6, 47.4, 31.7, 24.2, 23.8. HRMS (ESI, $\text{M} + \text{H}^+$) calcd for $\text{C}_{28}\text{H}_{31}\text{FN}_2\text{O}_2$: 447.2448; found: 447.2448. HPLC Purity: 96%; t_{R} 3.96 min.

2-(3-Chlorophenyl)-1-methyl-1-[4-(2-pyrrolidin-1-yl-ethoxy)phenyl]-1,2,3,4-tetrahydroisoquinolin-6-ol (19h). IR (KBr) ν_{max} : 3650–2100, 2971, 2907, 2810, 1610, 1585, 1506, 1468, 1243, 1227, 1181, 1072, 845, 790 cm^{-1} . ^1H NMR (400 MHz, DMSO) δ : 9.22 (s, 1H), 7.19 (d, $J = 8.5$ Hz, 2H), 7.04 (t, $J = 8.5$ Hz, 1H), 6.89–6.82 (m, 3H), 6.61–6.50 (m, 4H), 6.47 (dd, $J = 2.5, 8.5$ Hz, 1H), 4.07 (br s, 2H), 3.54–3.42 (m, 2H), 3.16–3.05 (m, 1H), 3.02–2.85 (m, 1H), 2.79 (dm, J for $d = 16.0$ Hz, 1H), 2.77–2.56 (m, 4H), 1.75 (br s, 4H), 1.66 (s, 3H). HRMS (ESI, $\text{M} + \text{H}^+$) calcd for $\text{C}_{28}\text{H}_{31}\text{ClN}_2\text{O}_2$: 463.2152; found: 463.2152. HPLC Purity: 95%; t_{R} 4.06 min.

2-(3-Chlorophenyl)-1-methyl-1-[4-(2-piperidin-1-yl-ethoxy)phenyl]-1,2,3,4-tetrahydroisoquinolin-6-ol (20h). IR (KBr) ν_{max} : 3650–2300, 1610, 1586, 1507, 1474, 1312, 1242, 1228, 1184, 1136, 1078, 846, cm^{-1} . ^1H NMR (400 MHz, DMSO) δ : 9.15 (s, 1H), 7.15 (d, $J = 9.0$ Hz, 2H), 7.02 (t, $J = 8.5$ Hz, 1H), 6.85 (d, $J = 8.5$ Hz, 1H), 6.81 (d, $J = 9.0$ Hz, 2H), 6.60–6.48 (m, 4H), 6.46 (dd, $J = 2.5, 8.5$ Hz, 1H), 4.02 (t, $J = 6.0$ Hz, 2H), 3.50–3.34 (m, 2H), 3.15–3.00 (m, 1H), 2.79 (dm, J for $d = 16.0$ Hz, 1H), 2.62 (t, $J = 6.0$ Hz, 2H), 2.47–2.31 (m, 4H), 1.64 (s, 3H), 1.54–1.42 (m, 4H), 1.42–1.29 (m, 2H). ^{13}C NMR (100.6 MHz, DMSO) δ : 156.9, 154.7, 151.7, 141.1, 134.9, 134.6, 132.2, 129.5, 129.0, 128.6, 122.9, 121.6, 120.9, 113.7, 113.7, 113.7, 65.5, 64.0, 57.3, 54.4, 45.5, 30.2, 25.5, 23.9, 22.9. HRMS (ESI, $\text{M} + \text{H}^+$) calcd for $\text{C}_{29}\text{H}_{33}\text{ClN}_2\text{O}_2$: 477.2309; found: 477.2308. HPLC Purity: 98%; t_{R} 4.43 min.

2-(3-Isopropylphenyl)-1-methyl-1-[4-(2-piperidin-1-yl-ethoxy)phenyl]-1,2,3,4-tetrahydroisoquinolin-6-ol (20i). IR (KBr) ν_{max} : 3600–2000, 2934, 2809, 1607, 1508, 1482, 1470, 1438, 1368, 1360, 1247, 1229, 1179, 1113, 842, 708 cm^{-1} . ^1H NMR (500 MHz, DMSO) δ : 9.17 (s, 1H), 7.08 (d, $J = 8.8$ Hz, 2H), 7.00 (t, $J = 7.8$ Hz, 1H), 6.78 (d, $J = 8.8$ Hz, 2H), 6.72 (d, $J = 7.8$ Hz, 1H), 6.60 (d, $J = 7.8$ Hz, 1H), 6.52 (d, $J = 8.5$ Hz, 1H), 6.50 (d, $J = 2.0$ Hz, 1H), 6.44 (dd, $J = 2.0, 8.5$ Hz, 1H), 6.15 (s, 1H), 4.02–3.94 (m, 2H), 3.50–3.40 (m, 1H), 3.30–3.23 (m, 1H), 3.12–3.02 (m, 1H), 2.77 (dm, J for $d = 16.0$ Hz, 1H), 2.62 (t, $J = 5.7$ Hz, 2H), 2.56 (septet, $J = 7.0$ Hz, 1H), 2.40 (br s, 4H), 1.54 (s, 3H), 1.52–1.44 (m, 4H), 1.40–1.32 (m, 2H), 0.93 (d, $J = 7.0$ Hz, 3H), 0.92 (d, $J = 7.0$ Hz, 3H). ^{13}C NMR (125.8 MHz, DMSO) δ : 156.9, 154.7, 150.3, 147.2, 141.6, 135.3, 134.9, 129.9, 129.2, 127.6, 123.3, 121.7, 120.7, 113.7, 113.6, 113.4, 65.5, 63.9, 57.4, 54.4, 45.6, 33.2, 30.6, 25.6, 24.0, 23.8, 23.6, 22.4. HRMS (ESI, $\text{M} + \text{H}^+$) calcd for $\text{C}_{32}\text{H}_{40}\text{N}_2\text{O}_2$: 485.3168; found: 485.3170. HPLC Purity: 100%; t_{R} 3.98 min.

2-(3-Dimethylaminophenyl)-1-methyl-1-[4-(2-pyrrolidin-1-yl-ethoxy)phenyl]-1,2,3,4-tetrahydroisoquinolin-6-ol (19j). IR (KBr) ν_{max} : 3600–2100, 2960, 2928, 1597, 1499, 1367, 1358, 1294, 1247, 1229, 1180, 1159, 806, 770 cm^{-1} . ^1H NMR

(500 MHz, DMSO) δ : 9.18 (s, 1H), 7.16 (d, $J = 8.8$ Hz, 2H), 6.90 (t, $J = 8.0$ Hz, 1H), 6.81 (d, $J = 8.8$ Hz, 2H), 6.52 (d, $J = 8.5$ Hz, 1H), 6.49 (d, $J = 2.3$ Hz, 1H), 6.43 (dd, $J = 2.3, 8.5$ Hz, 1H), 6.27 (dd, $J = 2.0, 8.0$ Hz, 1H), 6.16 (dd, $J = 1.2, 8.0$ Hz, 1H), 5.70 (s, 1H), 4.17–3.97 (m, 2H), 3.60–3.17 (m, 2H), 3.12–2.90 (m, 3H), 2.84–2.61 (m, 5H), 2.56 (s, 6H), 1.75 (br s, 4H), 1.56 (s, 3H). ^{13}C NMR (125.8 MHz, DMSO) δ : 156.5, 154.7, 151.0, 149.8, 142.55, 135.4, 134.9, 129.9, 129.2, 128.05, 113.7, 113.6, 113.5, 112.5, 110.4, 107.3, 65.8, 63.9, 53.9, 45.6, 30.55, 23.0, 22.5. HRMS (ESI, $\text{M} + \text{H}^+$) calcd for $\text{C}_{30}\text{H}_{37}\text{N}_3\text{O}_2$: 472.2964; found: 472.2957. HPLC Purity: 94%; t_{R} 3.56 min.

2-(3-Dimethylaminophenyl)-1-methyl-1-[4-(2-piperidin-1-yl-ethoxy)phenyl]-1,2,3,4-tetrahydroisoquinolin-6-ol (20j). IR (KBr) ν_{max} : 3650–2200, 2926, 2814, 1604, 1506, 1247, 1227, 1178, 849 cm^{-1} . ^1H NMR (500 MHz, DMSO) δ : 9.16 (s, 1H), 7.14 (d, $J = 8.5$ Hz, 2H), 6.90 (t, $J = 8.0$ Hz, 1H), 6.79 (d, $J = 8.5$ Hz, 2H), 6.52 (d, $J = 8.5$ Hz, 1H), 6.48 (d, $J = 2.0$ Hz, 1H), 6.43 (dd, $J = 2.0, 8.5$ Hz, 1H), 6.26 (dd, $J = 2.0, 8.0$ Hz, 1H), 6.16 (dd, $J = 1.0, 8.0$ Hz, 1H), 5.68 (br s, 1H), 4.08–3.94 (m, 2H), 3.45–3.37 (m, 1H), 3.31–3.24 (m, 1H), 3.11–3.02 (m, 1H), 2.75 (dm, J for $d = 16.0$ Hz, 1H), 2.70–2.57 (m, 2H), 2.55 (s, 6H), 2.50–2.34 (m, 4H), 1.56 (s, 3H), 1.54–1.44 (m, 4H), 1.42–1.32 (m, 2H). HRMS (ESI, $\text{M} + \text{H}^+$) calcd for $\text{C}_{31}\text{H}_{39}\text{N}_3\text{O}_2$: 486.3121; found: 486.3118. HPLC Purity: 92%; t_{R} 3.66 min.

Crystallography. The complex of ER α -LBD (Ser301 to Thr553) with **18a** was prepared as described previously.^{25,26} However, to overcome incomplete carboxymethylation of the free cysteines, a Cys \rightarrow Ser triple mutant of ER α -LBD (C381S, C417S, C530S) was expressed in *Escherichia coli* and purified to homogeneity by three-step chromatography. The crystals of ER α -LBD mutant in complex with **18a** were grown in a hanging drop vapor diffusion setup at room temperature. The reservoir buffer contained 100 mM MES buffer (pH = 6.5), 9–11% PEG-3350 and 400 mM NaCl. The protein solution contained 9.2 mg/mL ER α -LBD_{301–553}/mutant complex, 50 mM Tris buffer (pH = 8.0), 50 mM NaCl, 2 mM DTT, and 2 μM **18a**. The hanging drop was made by mixing 3 μL of protein solution and 1 μL of reservoir solution.

The crystals belong to the space group $P6_522$ and have unit cell dimensions of 58.2 Å, 58.2 Å and 274.6 Å. X-ray diffraction data to a resolution of 2.28 Å have been collected at 100 K at the “Swiss Norwegian Beam Line” at the ESRF in Grenoble with an R_{merge} of 5.3%. The data completeness was 77.8%. The structure was solved by molecular replacement using the coordinates of ER α -LBD (PDB accession number 3ERT)²⁶ as a starting model. The structure was refined to a crystallographic R -factor of 23.3% (R_{free} 28.7%). The root-mean-square deviations in bond length and bond angle are 0.007 Å and 1.1° respectively. (For details, see Supporting Information).

The structure factors and the coordinates of the refined structure were deposited in the protein structure database (PDB ID code: 1uom for the coordinate entry; r1uomsf for the structure factor entry).

Biological Assays. Radioligand Binding Studies. The radioligand binding assay was performed by using 96-well microtiterplates (Picroplates, Packard) in volumes of 0.2 mL of incubation buffer (50 mM Tris, pH 7.4). The incubation mixture contained 5 nM ER α (PanVera) or 6 nM ER β long form human recombinant receptors (PanVera), 8 nM [^3H] 17 β -estradiol (~180 000 total counts, Perkin-Elmer NET 517), the compound to be tested and 0.25 mg/well SPA-beads (Amersham RPNQ 0001). After incubation at rt for 2–4 h, the reaction was terminated by centrifugation at rt (10 min at 1000 g). The radioactivity was counted at least 3 h after completion of the experiment in a Packard Topcount scintillation counter. Nonspecific binding was defined as the remaining radioactivity in the presence of 10 μM nonradioactive 17 β -estradiol (Sigma). Assays were performed in triplicate.

MCF-7 Proliferation Assay. The human breast adenocarcinoma cell line, MCF-7 (ATCC HTB-22) was routinely cultivated in DMEM (Dulbecco's Modified Eagle medium High Glucose, Gibco Invitrogen Corporation, Paisley, U.K.) supplemented with 10% foetal bovine serum (FBS), 2 mM

L-glutamine, 10 mM Hepes (4-(2-hydroxyethyl)-1-piperazineethanesulfonic acid), 50 IU/mL penicillin, and 50 μ g/mL streptomycin (pen/strep) at 37 °C in a 5% CO₂ humidified incubator. Three days prior to an assay, MCF-7 cells were switched to DMEM Low Glucose phenol red-free²⁹ supplemented with 10% dextran-coated charcoal-stripped FBS (sFBS) to deplete internal stores of steroids, 2 mM L-glutamine, 10 mM Hepes, and pen/strep. Cells were trypsinized from the maintenance flask with phenol red-free trypsin (0.05%)–EDTA (0.02%) (HyClone, Logan, UT) and seeded in a 96-well plate (Nunc) at a density of 10³ cells per final volume of 100 μ L DMEM Low Glucose phenol red-free supplemented with 5% sFBS, 2 mM L-glutamine, 10 mM Hepes, and pen/strep. Twenty four hours later, fresh medium, supplemented with serial dilutions of compounds or DMSO as diluent control, was prepared and added in the presence or absence of 10⁻¹⁰ M 17 β -estradiol to triplicate microcultures. Cells were incubated for 6 days, and medium with compounds was changed once after 3 days. At the end of the incubation time, proliferation was assessed using the CellTiter 96 AQueous One Solution Cell Proliferation Assay kit from Promega (Madison, WI) according to the manufacturer's instructions. The absorbance at 490 nm was measured. This parameter relates to the amount of formazan produced,³⁰ the quantity of which is directly proportional to the number of living cells in the culture.

ERE-Luciferase Reporter Assay. HELN α and HELN β , two human cervix adenocarcinoma cell lines derived from HeLa cells stably transfected with the reporter gene ERE- β Glob-Luc-SVNeo (ERE, estrogen response element) and the expression plasmids ER α or ER β , respectively, were used to quantify the antiestrogenic and estrogenic effects of compounds on ERE.³¹ These cells were routinely cultivated in DMEM phenol red-free, supplemented with 5% sFBS, 2 mM glutamine, pen/strep, 1 mg/mL Geneticin and 0.5 μ g/mL puromycin to ensure appropriate antibiotic selection. For the assay, cells were trypsinized from the maintenance flask with phenol red-free trypsin (0.05%) – EDTA (0.02%) (HyClone, Logan, UT) and seeded in opaque 96-well plate (Nunc) at a density of 7.5 \times 10⁴ cells/well in a final volume of 100 μ L of assay medium (DMEM phenol red-free, supplemented with 3% sFBS, 2 mM glutamine and pen/strep). Five hours later, cells were adherent. Serial dilutions of compounds or DMSO as diluent control were then added in the presence of a fixed concentration of 17 β -estradiol (10⁻¹⁰ M in HELN α and 10⁻⁹ M in HELN β) to triplicate microcultures. Faslodex (Tocris, 10⁻⁸ M) was used as a baseline indicator. Cells were incubated for 20 h at 37 °C in a 5% CO₂ humidified incubator before being processed for luciferase determination. Medium was aspirated and 100 μ L of a 1:1 mixture of LucLite (Perkin-Elmer, Life Science, Boston, MA)/assay medium was added to each well. Plates were then left in the dark for 10 min before luminescence activity was determined by counting the plates for 6 s in a β -TopCount (Packard Instrument Company, Meriden, CT).

Cassette Dosing Experiments. Rat Pharmacokinetic Cassette Standard Assay. A set of seven novel compounds plus the internal standard raloxifene (5) was administered intravenously via the femoral vein at a dose level of 1 mg/kg body weight (for each individual compound) to four female rats. Cannulas were implanted into the femoral vein for intravenous compound administration and into the femoral artery for rapid blood sampling. Compounds were administered orally by gavage at a dose level of 5 mg/kg body weight. Blood was sampled over a 24 h time period postdose (from 5 min for iv and 15 min for po). Blood samples were then processed through steps involving protein precipitation by CH₃CN addition, centrifugation of the supernatant, and evaporation of the supernatant in a vacuum centrifuge. Dried residues were dissolved in MeOH/H₂O (60:40 v/v) containing 1% HCOOH and analyzed by HPLC on an Uptisphere C18 reversed-phase HPLC column (particle size: 3 μ m; column dimensions: 2 \times 50 mm). Eluents used consisted of A: 10% CH₃CN in H₂O with 0.1% HCOOH (pH 2.1); B: 90% CH₃CN with 10% H₂O and 0.1% HCOOH (pH 2.1). A linear gradient was run from 5 to 100% B over 7 min followed by a 3 min hold at 100% B at a

constant temperature of 50 °C in the column compartment. The flow rate was held constant at 0.4 mL/min. Sample injection volume was 10 μ L. The flow from the HPLC system was directly introduced into the ion source of an Agilent 1100 series MS-detector (single quadrupole mass analyzer) and subjected to atmospheric pressure electrospray ionization (positive mode). All compounds were detected as protonated quasi-molecular ions [M + H]⁺. A structurally closely related SERM was used as an analytical internal standard. Quantification of blood levels of the parent compounds was based on a 7-level calibration curve (in triplicate) using blank rat blood samples spiked with stock solutions of external and internal standards.

Rat Pharmacokinetic Cassette Validation. Raloxifene (5) alone was administered iv (1 mg/kg) and po (3 mg/kg) to four female rats each. Blood samples were taken and analyzed as described above. The pharmacokinetic data generated from this validation study were compared with those obtained for raloxifene (5) in cassette dosing experiments to check for potential pharmacokinetic interactions. Deviations exceeding the typical range of biological variability (approximately \pm 50% max. for individual parameters) were considered strongly indicative for pharmacokinetic interactions between compounds in the cassette, and the respective data were discarded.

Acknowledgment. We would like to thank our collaborators for their important contribution to the work disclosed herein: Nadine Braendlin, Patrick Lerch, Phillip Milnes, Pierre Martin, Nicole Reymann, Hans Rudolf Zihlmann, Diana Latscha, Roland Feifel, Jean-Louis Runser, Yves Seltenmeyer, Tanja Grabenstaetter and Erika Kuhn. In addition, the support of M. Geiser, M. Mahnke, and P. Graff for cloning, expression and mass spectrometry analysis of ER α -LBD and the experimental assistance from the staff of the Swiss-Norwegian Beam Lines at the European Synchrotron Radiation Facilities in Grenoble are gratefully acknowledged. We also wish to thank Drs. J-C. Nicolas and P. Balaguer (INSERM U439, Montpellier, France) for their precious advice on the use of the HELN α and HELN β cell lines and Drs. Juerg Gasser and Marc Gerspacher for their useful comments.

Supporting Information Available: Protein preparation, crystallization, data collection, structure resolution, and docking/modeling studies. This material is available free of charge via the Internet at <http://pubs.acs.org>.

References

- (1) Eriksen, E. F.; Axelrod, D. W.; Melsen, F. *Bone Histomorphometry*. Raven Press: New York, 1994; pp 3–12.
- (2) Rickard, D. J.; Subramaniam, M.; Spelsberg, T. C. *Molecular and Cellular Mechanisms of Estrogen Action on the Skeleton*. *J. Cell. Biochem.* **1999**, *S32/S33*, 123–132.
- (3) (a) Dechering, K.; Boersma, C.; Mosselman, S. Estrogen Receptors α and β : Two Receptors of a Kind? *Curr. Med. Chem.* **2000**, *7*, 561–576; (b) Mosselman, S.; Polman, J.; Dijkema, R. ER β : Identification and Characterization of a Novel Human Estrogen Receptor. *FEBS Lett.* **1996**, *392*, 49–53.
- (4) (a) Taylor, A. H.; Al-Azzawi, F. Immunolocalisation of Oestrogen Receptor Beta in Human Tissues. *J. Mol. Endocrinol.* **2000**, *24*, 145–155 and references therein.
- (5) Pike, A. C. W.; Brzozowski, A. M.; Hubbard, R. E.; Bonn, T.; Thorsell, A.-G.; Engström, O.; Ljunggren, J.; Gustafsson, J.-Å.; Carlquist, M. Structure of the Ligand-Binding Domain of Oestrogen Receptor Beta in the Presence of a Partial Agonist and a Full Antagonist. *EMBO J.* **1999**, *18*, 4608–4618.
- (6) (a) Bilezikian, J. P. Sex Steroids, Mice and Men: When Androgens and Estrogens Get Very Close to Each Other. *J. Bone Miner. Res.* **2002**, *17*, 563–566; (b) Sims, N. A.; Dupont, S.; Krust, A.; Clement-Lacroix, P.; Minet, D.; Resche-Rigon, M.; Gaillard-Kelly, M.; Baron, R. Deletion of Estrogen Receptors Reveals a Regulatory Role for Estrogen Receptors- β in Bone Remodeling in Females but Not in Males. *Bone* **2002**, *30*, 18–25.

- (7) (a) Sato, M.; Grese, T. A.; Dodge, J. A.; Bryant, H. U.; Turner, C. H. Emerging Therapies for the Prevention or Treatment of Postmenopausal Osteoporosis. *J. Med. Chem.* **1999**, *42*, 1–24. (b) Kanis, J. A. Estrogens, the Menopause, and Osteoporosis. *Bone* **1996**, *19*, 185S–190S.
- (8) (a) Torgerson, D. J. HRT and its Impact on the Menopause, Osteoporosis and Breast Cancer. *Exp. Opin. Pharmacother.* **2000**, *1*, 1163–1169. (b) Palacios, S. Current Perspectives on the Benefits of HRT in Menopausal Women. *Maturitas* **1999**, *33*, S1–S13.
- (9) Writing Group for the Women's Health Initiative Investigators. Risks and Benefits of Estrogen Plus Progestin in Healthy Postmenopausal Women. *JAMA* **2002**, *288*, 321–333.
- (10) For recent reviews about SERMs, see: (a) Miller, C. P. SERMs: Evolutionary Chemistry, Revolutionary Biology. *Curr. Pharm. Des.* **2002**, *8*, 2089–2111. (b) Labrie, F.; Labrie, C.; Bélanger, A.; Giguere, V.; Simard, J.; Mérand, Y.; Gauthier, S.; Luu-The, V.; Candas, B.; Martel, C.; Luo, S. Pure Selective Estrogen Receptor Modulators, New Molecules Having Absolute Cell Specificity Ranging from Pure Antiestrogenic to Complete Estrogen-Like Activities. *Adv. Protein Chem.* **2001**, *56*, 293–369. (c) Dutertre, M.; Smith, C. L. Molecular Mechanisms of Selective Estrogen Receptor Modulator (SERM) Action. *J. Pharmacol. Exp. Ther.* **2000**, *295*, 431–437 and references therein; (d) McDonnell, D. P. The Molecular Pharmacology of SERMs. *TEM* **1999**, *10*, 301–311 and references therein.
- (11) Maricic, M.; Gluck, O. Review of Raloxifene and its Clinical Applications in Osteoporosis. *Expert Opin. Pharmacother.* **2002**, *3*, 767–775
- (12) White, I. N. H. The Tamoxifen Dilemma. *Carcinogenesis* **1999**, *20*, 1153–1160.
- (13) Grese, T. A.; Sluka, J. P.; Bryant, H. U.; Cullinan, G. J.; Glasebrook, A. L.; Jones, C. D.; Matsumoto, K.; Palkowitz, A. D.; Sato, M.; Termine, J. D.; Winter, M. A.; Yang, N. N.; Dodge, J. A. Molecular Determinants of Tissue Selectivity in Estrogen Receptor Modulators. *Proc. Natl. Acad. Sci. U.S.A.* **1997**, *94*, 14105–14110.
- (14) Rosati, R. L.; Jardine, P. Da Silva; Cameron, K. O.; Thompson, D. D.; Ke, H. Z.; Toler, S. M.; Brown, T. A.; Pan, L. C.; Ebbinghaus, C. F.; Reinhold, A. N.; Elliott, N. C.; Newhouse, B. N.; Tjoa, C. M.; Sweetnam, P. M.; Cole, M. J.; Arriola, M. W.; Gauthier, J. W.; Crawford, D. T.; Nickerson, D. F.; Pirie, C. M.; Qi, H.; Simmons, H. A.; Tkalcevic, G. T. Discovery and Preclinical Pharmacology of a Novel, Potent, Nonsteroidal Estrogen Receptor Agonist/Antagonist, CP-336156, a Diaryltetrahydro-naphthalene. *J. Med. Chem.* **1998**, *41*, 2928–2931. In addition, raloxifene possesses two phenolic OHs, both of which undergo glucuronidation, see: Dodge, J. A.; Lugar, C. W.; Cho, S.; Short, L. L.; Sato, M.; Yang, N. N.; Spangle, L. A.; Martin, M. J.; Phillips, D. L.; Glasebrook, A. L.; Osborne, J. J.; Frolik, C. A.; Bryant, H. U. Evaluation of the Major Metabolites of Raloxifene as Modulators of Tissue Selectivity. *J. Steroid Biochem. Mol. Biol.* **1997**, *61*, 97–106.
- (15) A similar route using intermediates with different protecting groups has been reported: Nagarajan, K.; Talwalker, P. K.; Kulkarni, C. L.; Shah, R. K.; Shenoy, S. J.; Prabhu, S. S. Antiimplantation Agents: Part II 1,2-Diaryl-1,2,3,4-tetrahydroisquinolines. *Indian J. Chem.* **1985**, *24B*, 83–97.
- (16) Ohkubo, M.; Kuno, A.; Katsuta, K.; Ueda, Y.; Shirakawa, K.; Nakanishi, H.; Nakanishi, I.; Kinoshita, T.; Takasugi, H. Studies on Cerebral Protective Agents. IX. Synthesis of Novel 1,2,3,4-Tetrahydroisquinolines as *N*-Methyl-D-Aspartate Antagonists. *Chem. Pharm. Bull.* **1996**, *44*, 95–102.
- (17) (a) Shanker, P. S.; Subba Rao, G. S. R. Synthesis of Isoquinolines from Indanones: Total Synthesis of Illudinine. *Indian J. Chem., Sect. B*, **1993**, *32B*, 1209–1213. (b) earlier reports had demonstrated that the methoxy group para to the carbonyl functionality of the indanone favors the migration of the alkyl over the aryl substituent in the presence of sulfuric acid, see: Tomita, M.; Minami, S.; Uyeo, S. The Schmidt Reaction with Benzocycloalkenones. *J. Chem. Soc. C* **1969**, 183–188.
- (18) Sugahara, M.; Ukita, T. A Facile Copper-Catalyzed Ullmann Condensation: *N*-Arylation of Heterocyclic Compounds Containing an –NHCO– Moiety. *Chem. Pharm. Bull.* **1997**, *45*, 719–721.
- (19) Akiyama, T.; Hirofuji, H.; Ozaki, S. AlCl₃-*N,N*-Dimethyl-aniline: A New Benzyl and Allyl Ether Cleavage Reagent. *Tetrahedron Lett.* **1991**, *32*, 1321–1324.
- (20) (a) The methoxy analogues of **17a** and **18a** were disclosed in an earlier publication, the pyrrolidinoethoxy derivative showing antiimplantation activity while the piperidinoethoxy analogue did not. See ref 15. (b) Tetrahydroisquinoline **17a** was previously reported in the patent literature as an estrogenic agent. The biological data for this compound were not disclosed however. See: Cameron, K. O.; Jardine, P. A. DaSilva. Preparation of 5-[4-(2-heterocyclolethoxy)phenyl]-5,6,7,8-tetrahydronaphthalene-2-ols and 1-[4-(2-heterocyclolethoxy)phenyl]-6-hydroxy-1,2,3,4-tetrahydroisquinolines as estrogen agonists/antagonists. PCT Int. Appl. WO 9621656, 1996.
- (21) Dukes, M.; Chester, R.; Yarwood, L.; Wakeling, A. E. Effects of a Non-Steroidal Pure Antioestrogen, ZM 189, 154, on Oestrogen Target Organs of the Rats Including Bones. *J. Endocrinol.* **1994**, *141*, 335–341.
- (22) (a) Grese, T. A.; Adrian, M. D.; Phillips, D. L.; Shetler, P. K.; Short, L. L.; Glasebrook, A. L.; Bryant, H. U. Photochemical Synthesis of *N*-Arylbenzophenanthridine Selective Estrogen Receptor Modulators (SERMs). *J. Med. Chem.* **2001**, *44*, 2857–2860. (b) Grese, T. A.; Cho, S.; Finley, D. R.; Godfrey, A. G.; Jones, C. D.; Lugar, C. W., III; Martin, M. J.; Matsumoto, K.; Pennington, L. D.; Winter, M. A.; Adrian, M. D.; Cole, H. W.; Magee, D. E.; Phillips, D. L.; Rowley, E. R.; Short, L. L.; Glasebrook, A. L.; Bryant, H. U. Structure–Activity Relationships of Selective Estrogen Receptor Modulators: Modifications to the 2-Arylbenzothiophene Core of Raloxifene. *J. Med. Chem.* **1997**, *40*, 146–167.
- (23) Shang, Y.; Brown, M. Molecular Determinants for the Tissue Specificity of SERMs. *Science* **2000**, *295*, 2465–2468.
- (24) (a) Labrie, F.; Labrie, C.; Bélanger, A.; Simard, J.; Gauthier, S.; Luu-The, V.; Mérand, Y.; Giguere, V.; Candas, B.; Luo, S.; Martel, C.; Singh, S. M.; Fournier, M.; Coquet, A.; Richard, V.; Charbonneau, R.; Charpenet, G.; Tremblay, A.; Tremblay, G.; Cusan, L.; Veilleux, R. EM-652 (SCH 57068), a Third Generation SERM Acting As Pure Antiestrogen in the Mammary Gland and Endometrium. *J. Steroid Biochem. Mol. Biol.* **1999**, *69*, 51–84 and references therein. (b) Poulin, R.; Mérand, Y.; Poirier, D.; Lévesque, C.; Dufour, J. M.; Labrie, F. Antiestrogenic Properties of Keoxifene, Trans-4-Hydroxytamoxifen, and ICI 164384, a New Steroidal Antiestrogen, in ZR-75–1 Human Breast Cancer Cells. *Breast Cancer Res. Treat.* **1989**, *14*, 65–76. (c) DeFriend, D. J.; Anderson, E.; Bell, J.; Wilks, D. P.; West, C. M.; Mansel, R. E.; Howell, A. Effects of 4-Hydroxytamoxifen and a Novel Pure Antioestrogen (ICI 182780) on the Clonogenic Growth of Human Breast Cancer Cells in Vitro. *Br. J. Cancer* **1994**, *70*, 204–211. (d) Reddel, R. R.; Sutherland, R. L. Tamoxifen Stimulation of Human Breast Cancer Cell Proliferation in Vitro: A Possible Model for Tamoxifen Tumour Flare. *Eur. J. Cancer Clin. Oncol.* **1984**, *20*, 1419–1424.
- (25) Brzozowski, A. M.; Pike, A. C. W.; Dauter, Z.; Hubbard, R. E.; Bonn, T.; Engström, O.; Ohman, L.; Greene, G. L.; Gustafsson, J.-Å.; Carlquist, M. Molecular Basis of Agonism and Antagonism in the Oestrogen Receptor. *Nature* **1997**, *389*, 753–758.
- (26) Shiau, A. K.; Barstad, D.; Loria, P. M.; Cheng, L.; Kushner, P. J.; Agard, D. A.; Greene, G. L. The Structural Basis of Estrogen Receptor/Coactivator Recognition and the Antagonism of this Interaction by Tamoxifen. *Cell* **1998**, *95*, 927–937.
- (27) The crystal structure of a triple cysteine to serine mutant ER α -LBD complexed with estradiol was reported prior to our work. See: Gangloff, M.; Ruff, M.; Eiler, S.; Duclaud, S.; Wurtz, J.-M.; Moras, D. Crystal Structure of a Mutant hER α Ligand-Binding Domain Reveals Key Structural Features for the Mechanism of Partial Agonism. *J. Biol. Chem.* **2001**, *276*, 15059–15065.
- (28) (a) Bury, P. S.; Christiansen, L. B.; Jacobsen, P.; Jørgensen, A. S.; Kanstrup, A.; Naerum, L.; Bain, S.; Fledelius, C.; Gissel, B.; Hansen, B. S.; Korsgaard, N.; Thorpe, S. M.; Wassermann, K. Synthesis and Pharmacological Evaluation of Novel *cis*-3,4-Diaryl-hydroxychromanes as High Affinity Partial Agonists for the Estrogen Receptor. *Bioorg. Med. Chem.* **2002**, *10*, 125–145. (b) Gauthier, S.; Caron, B.; Cloutier, J.; Dory, Y. L.; Favre, A.; Larouche, D.; Mailhot, J.; Ouellet, C.; Schwerdtfeger, A.; Leblanc, G.; Martel, C.; Simard, J.; Mérand, Y.; Bélanger, A.; Labrie, C.; Labrie, F. (S)-(+)-4-[7-(2,2-Dimethyl-1-oxopropoxy)-4-methyl-2-[4-[2-(1-piperidinyl)ethoxy]phenyl]-2H-1-benzopyran-3-yl]-phenyl]-2,2-Dimethylpropanoate (EM-800): A Highly Potent, Specific, and Orally Active Nonsteroidal Antiestrogen. *J. Med. Chem.* **1997**, *40*, 2117–2122.
- (29) Berthois, Y.; Katzenellenbogen, J. A.; Katzenellenbogen, B. S. Phenol Red in Tissue Culture Media is a Weak Estrogen: Implications Concerning the Study of Estrogen-Responsive Cells in Culture. *Proc. Natl. Acad. Sci. U.S.A.* **1986**, *83*, 2496–2500.
- (30) This assay solution contains PES (phenazine ethosulfate), an electron coupling reagent and MTS (3-(4,5-dimethylthiazol-2-yl)-5-(3-carboxymethoxyphenyl)-2-(4-sulfophenyl)-2H-tetrazolium or Owen's reagent). MTS is bioreduced by the cells into a coloured formazan product soluble in the culture medium.
- (31) (a) Balaguer, P.; Boussioux, A.-M.; Demirpençe, E.; Nicolas, J.-C. Reporter Cell Lines are Useful Tools for Monitoring Biological Activity of Nuclear Receptor Ligands. *Luminescence* **2001**, *16*, 153–158; (b) Balaguer, P.; Francois, F.; Comunale, F.; Fenet, H.; Boussioux, A.-M.; Pons, M.; Nicolas, J.-C. and Casellas, C. Reporter Cell Lines to Study the Estrogenic Effects of Xenestrogens. *Sci. Total Environ.* **1999**, *233*, 47–56.